



Słowakiewicz, M., Tucker, M. E., Hindenberg, K., Mawson, M., Idiz, E. F., & Pancost, R. D. (2016). Nearshore euxinia in the photic zone of an ancient sea: Part II – The bigger picture and implications for understanding ocean anoxia. *Palaeogeography, Palaeoclimatology, Palaeoecology*, 461, 432-448.
<https://doi.org/10.1016/j.palaeo.2016.09.003>

Peer reviewed version

License (if available):
CC BY-NC-ND

Link to published version (if available):
[10.1016/j.palaeo.2016.09.003](https://doi.org/10.1016/j.palaeo.2016.09.003)

[Link to publication record in Explore Bristol Research](#)
PDF-document

This is the accepted author manuscript (AAM). The final published version (version of record) is available online via Elsevier at <http://dx.doi.org/10.1016/j.palaeo.2016.09.003>. Please refer to any applicable terms of use of the publisher.

University of Bristol - Explore Bristol Research

General rights

This document is made available in accordance with publisher policies. Please cite only the published version using the reference above. Full terms of use are available:
<http://www.bristol.ac.uk/red/research-policy/pure/user-guides/ebr-terms/>

Nearshore euxinia in the photic zone of an ancient sea: Part II – the bigger picture and implications for understanding ocean anoxia

Mirosław Słowakiewicz^{1,2,3}, Maurice E. Tucker^{3,4}, Katja Hindenberg⁵, Mike Mawson⁶, Erdem F. Idiz⁷, Richard D. Pancost^{1,3}

¹Organic Geochemistry Unit, School of Chemistry, University of Bristol, Cantock's Close, BS8 1TS, United Kingdom; e-mail: m.slowakiewicz@gmail.com

²Polish Geological Institute, Rakowiecka 4, 00-975 Warszawa, Poland

³Cabot Institute, University of Bristol, Cantock's Close, Bristol, BS8 1UJ, UK

⁴Department of Earth Sciences, University of Bristol, Bristol, BS8 1RJ, UK

⁵Institute of Bio- and Geosciences (IBG-3), Forschungszentrum Jülich GmbH, D-52425 Jülich, Germany

⁶Department of Earth Sciences, Durham University, Durham, DH1 3LE, UK

⁷Department of Earth Sciences, University of Oxford, South Parks Road, Oxford, OX1 3AN, UK

Highlights

- A shelf to basin reconstruction of redox conditions
- Spatial variations in facies and oceanographic conditions
- Euxinia in marginal locations is not associated with widespread basin-scale anoxia
- A model of spatially heterogeneous anoxia is presented
- Implications for understanding ocean anoxia at other times

Abstract

Biomarker, palaeontological and isotopic evidence suggests that the Late Permian carbonate seas, i.e. the Northern (NPB) and Southern (SPB) Permian basins of northern Pangea, were characterized by significant spatial and temporal variations in the palaeowater-column redox state. This is particularly the case with regards to the deposition of the Lopingian Zechstein cycle 2 carbonate rocks. A shelf to basin reconstruction of environmental conditions was achieved by analysing nearly 400 core samples from 49 wells. This allowed an evaluation of the spatial variations in facies and broad oceanographic conditions at the basin scale. Specifically, in the lower slope and shallow-basin facies of the northern margin of the SPB (present-day northern Poland and eastern Germany), highly variable concentrations of the green sulphur bacterial biomarkers chlorobactane and isorenieratane (and their likely degradation products, C₁₅ to C₃₁ 2,3,6-aryl isoprenoids, indicative of photic zone euxinia) and homohopane indices (indicative of anoxia), combined with the presence of a benthic fauna and bioturbation, indicate a variable but occasionally anoxic/euxinic water column. Locally in lagoonal facies in the northern and southern margin of the SPB, euxinic conditions also developed but these were likely associated with localised conditions or benthic production in association with microbialites. The presence of gammacerane in the eastern SPB (south-eastern Germany and eastern Poland) suggests elevated salinities there, compatible with the restricted configuration of the basin. However, a lack of these signatures in basinal settings of the eastern SPB indicates that strongly reducing conditions were restricted to the lower slope and shallow-basin locations and restricted lagoons, and were not developed in the basin centre. Moreover, this anoxia/euxinia in marginal settings is restricted to the north-eastern part of the SPB. The south-eastern part of the SPB (SE Poland), in contrast, is devoid of evidence for PZE. The southern margin of the SPB is also characterized by generally oxic-

suboxic conditions, with local anoxia limited to more restricted embayments, and elevated salinities limited to restricted oxic-anoxic lagoons. In the western SPB (NE England and adjacent offshore) and the NPB (Outer Moray Firth, offshore Scotland) the water columns were oxic-suboxic. Overall, it appears that high but episodic primary bioproductivity of organic matter was concentrated on (or even limited to) the lower slopes of the SPB's north-eastern margin and the restricted lagoons and shallow basin of its southern margin, leading to the formation of source rocks for petroleum in these areas. In addition, the temporal and geographical restriction of anoxia appears to have prevented the accumulation of large and more widespread quantities of organic matter; in fact TOC contents exhibit a poor correlation with ecological and anoxia indicators. Crucially, this work confirms that the strong evidence for PZE observed in shelf and lower slope/shallow-basin facies of the north-eastern SPB need not be associated with widespread, basin-scale anoxia; this conclusion has implications for organic matter burial, carbon cycling and biotic crises during other times in Earth history.

Keywords: nearshore euxinia, anoxia, lipid biomarkers, organic matter, carbonate rocks, Zechstein, Late Permian

1. Introduction

The geographical distribution of O₂ in the marine water column is governed by a wide range of controls, including climate, nutrient supply, molecular diffusion, photosynthesis, respiration, global ocean circulation, localised upwelling and downwelling processes, and the configuration of the basin (e.g., Canfield et al., 2005). These govern O₂ content and organic

matter (OM) burial via their impact on bioproductivity, the biological pump, sediment deposition, and deep water ventilation (Ducklow and Steinberg, 2001; Hain et al., 2014).

Processes other than anoxia and productivity which have been invoked to modulate the preservation potential of OM include sedimentation rate (Müller and Suess, 1979; Henrichs, 1992), grain size (Bergamaschi et al., 1997), mineral adsorption (Mayer, 1994), and anaerobic respiration. The last might be as effective in OM recycling as oxic metabolic pathways (Canfield, 1994).

The relative influence of factors controlling O₂ distribution and OM burial has been widely debated (e.g., Sarmiento et al., 1988; Pedersen and Calvert, 1990; Canfield, 1994; Hedges and Keil, 1995; Mayer, 1995; Tyson, 1995; Kenig et al., 2004; Kuypers et al., 2004a; Jenkyns, 2010), but today water column anoxia is largely restricted to oxygen minimum zones which form beneath areas of high productivity. Anoxia also occurs in chemically-stratified epeiric basins, such as the modern Black Sea where euxinic conditions extend into the photic zone (Overmann et al., 1992; Repeta, 1993; Sinninghe Damsté et al., 1993). The Black Sea model has been directly invoked as an analogue for ancient euxinic basins (Arthur and Sageman, 1994), and it is implicitly invoked when observations of anoxia in marginal settings are extrapolated to infer basin-scale anoxia (Joachimski et al., 2001; Grice et al., 2005). Although geochemical records of some Mesozoic oceanic anoxic events (OAEs) suggest that ocean anoxia does extend into deep basins (Sinninghe Damsté and Köster, 1998; Wagner et al., 2004; Pancost et al., 2002; van Breugel et al., 2006), recent work suggests that this was not necessarily associated with basin-scale stratification (Kuypers et al., 2002, 2004a,b; Monteiro et al., 2012). Moreover, the evidence for anoxia in many ancient basins is interpreted as restricted to nearshore settings (e.g. Jenkyns, 1985, 1988; Wignall and Newton, 2001). Crucially, some of these authors have invoked a counter-model to the Black Sea – the bath-tub ring model of deposition in which anoxia in stratified basins is largely restricted to

nearshore settings (Frakes and Bolton, 1984; Wignall and Newton, 2001). Both models are useful for extrapolating spatially limited geological data, especially in Palaeozoic settings, to infer larger-scale basinal characteristics. However, those respective interpretations have vastly different implications for understanding past environmental changes, biotic crises and source rock formation.

Here, we explore these models using organic geochemical analyses of over 400 rocks from 49 boreholes, collected from the Southern and Northern Permian basins of northern Europe. The Late Permian is characterised by a greenhouse climate with a vast intra-continental desert, an absence of polar ice-caps and average temperatures being more than 15°C higher than today (Khmel and Shields, 2005; Roscher et al., 2011). Such climatic conditions, as well as the restricted character of tectonic depressions largely fed by seawater and their subtropical location, favoured the formation of carbonate and evaporite sediments in many epeiric seas in the northern hemisphere, including the Northern Permian (NPB) and Southern Permian (SPB) basins in NW Europe. However, although extensively studied, the controversy and speculation towards the overall biogeochemistry and organic matter (OM) productivity of the basins in Lopingian (Zechstein) time still remain. It has long been thought that the Zechstein water-column was salinity stratified with anoxic bottom waters (Brongersma-Sanders, 1971; Turner and Magaritz, 1986; Grotzinger and Knoll, 1995; Taylor, 1998). Although it is well established that the initial transgressive lowermost Zechstein mudrock (Kupferschiefer, i.e., base of the first Zechstein cycle, Z1, Fig. 2) was deposited under such conditions with euxinia extending into the photic-zone (Oszczepalski, 1989; Schwark and Püttmann, 1990; Gibbison et al., 1995; Grice et al., 1996a,b, 1997; Pancost et al., 2002; Paul, 2006), the subsequent deposition of carbonate and evaporite sediments of the Z1 took place under varied oxic/suboxic to anoxic bottom-water conditions (Kluska et al., 2013; Peryt et al., 2015; Słowakiewicz et al., 2015). This clearly shows that the

epicontinental Zechstein Sea experienced euxinia periodically in the Z1 cycle, but it remains unclear as to how extensive this was spatially and what governed the apparently pronounced temporal variations in this and the Z2 and Z3 cycles.

Our previous shelf-to-basin reconstruction of environmental conditions in the Polish sector of the SPB in Europe has shown that euxinic conditions were present during the deposition of lower slope carbonate strata on the SPB northeast margin during deposition of the Zechstein second carbonate cycle (Ca2) (Słowakiewicz et al., 2015). However, initial data from the basinal facies suggested that the euxinic conditions did not develop there, but only in the nearshore environments, thus not on a basin-wide scale. This initial study, therefore, indicated that a restricted epeiric basin, i.e. a Black Sea analogue, is not appropriate to understand the SPB.

To explore this further and to test whether the rest of the basin and other marginal settings were also oxygenated – despite the strong evidence for photic zone euxinia (PZE) in the north-eastern SPB (NW Poland) – we examined the Ca2 cycle further. Our new data include sediments deposited in the NPB and the western, southern and south-eastern parts of the SPB, allowing a detailed examination of spatial (both basin- and facies- scale) variations in organic matter source and depositional conditions. We have quantified derivatives of isorenieratene and chlorobactene, which are produced by the brown and green strains of photosynthetic anaerobic green sulphur bacteria (*Chlorobiaceae*), respectively, allowing us to assess the geographical occurrence of photic zone euxinia and assess models for basin oceanography and redox conditions. These data and interpretations are complemented by other biomarker signatures indicative of past redox and other environmental conditions (homohopane ratios, bisnorhopane and gammacerane abundances) and changes in OM source (hopane and sterane distributions). These, as well as palaeontological and carbon and oxygen

isotopic data, are used to infer the connectivity of the NPB and SPB to the global ocean and to refine further basin-scale interpretations of productivity and anoxia.

2. Geological setting

Both the NPB and SPB were formed in the Late Carboniferous-Early Permian (Gast, 1988) and were located in the arid subtropical belt of Northern Pangea (Henderson and Mei, 2000; Legler and Schneider, 2008), at 15-20°N palaeolatitude, northwest of the Palaeo-Tethys Ocean, and south of the Boreal Sea (Fig. 1a). During the early Zechstein marine transgression (mid-latest Wuchiapingian, Szurliés, 2013), the subsiding basin was flooded with seawater from the Panthalassa Ocean entering through the Boreal Sea and a narrow strait between Greenland and Scandinavia, to form the vast epicontinental Zechstein Sea. The shallow sea (<350 m deep) is segmented into the NPB and SPB, partially separated by a series of Carboniferous palaeohighs, the Mid North Sea High and Ringkøbing-Fyn High (Fig. 1b). Both basins are of economic importance, containing a number of significant petroleum accumulations, mostly located in the SPB in what is today Germany, the Netherlands and Poland. The SPB comprises a series of connected sub-basins extending from eastern England across the North Sea into Poland and southern Lithuania, a distance of some 1700 km. Its width ranges from 300 to 600 km (Van Wees et al., 2000). The SPB had several narrow connections with adjacent basins (Sørensen and Martinsen, 1987) and possibly temporary connections with the Tethys domain to the southeast via the Polish-Dobrogea trough along a rift zone (Peryt and Peryt, 1977; Ziegler et al., 1997; Şengor and Atayman, 2009) and with small basins in the Inner Variscan domain (Kiersnowski et al., 1995) (Fig. 1). The sediments of the NPB were deposited in a smaller basin, located to the north of the Ringkøbing-Fyn

High, which was connected to the SPB via the Bamble and Glückstadt troughs and the Central and Horn grabens, among others (Stemmerik et al., 2000; Glennie et al., 2003).

The SPB was subject to periodic intense evaporation. Up to seven (Z1-Z7) evaporitic cycles have been recognized in different parts of the basins and the 2nd cycle carbonate (Ca2, ca. 254 Ma, Szurlies, 2013) is the most important hydrocarbon reservoir. Equivalents of the Ca2 are the Main Dolomite in Poland, Hauptdolomit in Germany (also Staßfurt Karbonat), the Netherlands and southern North Sea, the Roker Formation and Kirkham Abbey Formation in eastern England, and the Innes Carbonate offshore Scotland. Thin anhydrite and thick halite occur above (and below) the Ca2, creating a cap-rock for petroleum reservoirs (for lithostratigraphy see Słowakiewicz et al., 2015).

3. Samples and lithology

The well-established facies model for the Ca2 in the SPB is comprised of a shallow-water carbonate platform with interior peritidal flat – evaporitic sabkha, an extensive shallow-water lagoon and platform-margin oolite shoal and microbialites, passing basinwards through slope, toe-of-slope (lower slope), shallow basin, and basin-plain environments (Strohmenger et al., 1996, Słowakiewicz et al., 2013, 2015). The SPB was likely affected by locally and temporally punctuated freshwater pulses, resulting from strong summer monsoonal rains (Gąsiewicz, 2013 and references within).

In addition to the 150 borehole and well samples studied and reported in Słowakiewicz et al. (2015), we have collected and analysed another 264 samples, collectively comprising all the main Ca2 facies from the English, German and Polish parts of the NPB and SPB (Fig. 1b). Specifically, they were taken from basinal (well Florentyna IG-2), outer shelf and upper slope (well A, Bates Colliery B2 and B8), middle slope (wells: E, Vane Tempest VT-11), lower

slope (wells B, C, Gomunice-10, Gorzów Wielkopolski-2, Lockton-2a and -7, Egton High Moor-1), oolite shoal (wells: D, F), and lagoonal lithofacies (wells: G, H, I, J, Malton-1 and -4, Miłów-1, Ettrick 20/2-2, Offshore Borehole-1). In addition, published geochemical data from Aue 1 slope lithofacies (Hofmann and Leythaeuser, 1995), Dachwig 1/70 and 2/71, Jena 106/62, Tennstedt 1/69 lagoonal lithofacies, Eckartsberga 1/68 and 2/68, Mellingen 1/70 slope lithofacies, Straußfurt 8/70 slope/oolite shoal lithofacies, Sprötau 4/69 basin facies (Slach, 1993), and Sprötau Z1 slope lithofacies (Schwark et al., 1998) are utilised. Selected wells and their facies are presented in Figure 2 and 3.

4.Methods

4.1. Carbon and oxygen stable isotopes

100-200 µg of powdered carbonate were placed into 4 ml glass vials, and then sealed by a lid and pierceable septum. The vials were placed in a heated sample rack (90°C) where the vial head space was replaced by pure helium via an automated needle system as part of an Isoprime Multiflow preparation system. Samples were then manually injected with approximately 200 µl of phosphoric acid and left to react for at least 1.5 hrs before the headspace gas was sampled by automated needle and introduced into a continuous-flow Isoprime mass-spectrometer. Duplicate samples were extracted from each vial, and a mean value obtained for both $\delta^{13}\text{C}$ and $\delta^{18}\text{O}$. Samples were calibrated using IAEA standards NBS-18 and NBS-19, and reported as ‰ on the VPDB scale. Reproducibility within runs was 0.09 ‰ $\delta^{18}\text{O}$ and 0.05 ‰ $\delta^{13}\text{C}$.

4.2. Total organic carbon (TOC) contents

Two hundred and sixty four total carbon ($\pm 0.2\%$) contents were obtained from the powdered samples using EuroVector EA3000 and LECO Elemental Analysers. Total

inorganic carbon was determined (± 0.1 %) as carbonate using a CO₂ coulometer (a modified Ströhlein Coulomat 702 Analyser). Total organic carbon (TOC) contents were calculated as the difference between total carbon and total inorganic carbon.

4.3. Sample extraction and fractionation

Two hundred and sixty four powdered (20 g) core samples were extracted using a Soxhlet apparatus with 200-mL dichloromethane:methanol (9:1, vol./vol.) for 24 hr; copper was added to the round-bottom flask to remove elemental sulphur. Aliquots of total lipid extract were separated into apolar, aromatic and polar fractions using a column with activated silica gel (230–400 mesh; 4 cm bottom). Elution proceeded with 3 mL of hexane (saturated fraction), 3 mL of hexane:dichloromethane (3:1, vol/vol; aromatic fraction), and 5 mL of methanol (polar fraction). Among the lipids extracted from the analysed samples only compounds detected in saturated and aromatic fractions are reported here. Polar compounds were not detected in samples from basinal facies.

4.4. Gas chromatography-mass spectrometry (GC-MS)

Aliquots (1 mL) of each fraction were analysed by gas chromatography (GC) using a Hewlett Packard 5890 Series II instrument, fitted with an on-column injector and a capillary column with a CP Sil5-CB stationary phase (60 m \times 0.32 mm; df = 0.10 μ m). Detection was achieved with flame ionization, with helium as the carrier gas. The temperature program consisted of three stages: 70°–130°C at 20°C per minute; 130°–300°C at 4°C per minute; and 300°C at which the temperature was held for 10 min. Gas chromatography–mass spectrometry analyses were performed using a ThermoQuest Finnigan Trace GC–mass spectrometer fitted with an on-column injector and using the same column and temperature

program as for GC analyses. The detection was based on electron ionization (source at 70 eV; scanning range, 50–580 Da), and compounds were identified by comparison of retention times and mass spectra to the literature. Individual compounds were identified and quantified relative to internal standards (octatriacontane).

5. Results

5.1. Total organic carbon content and thermal maturity

The compilation of TOC contents from this and numerous previous studies (e.g., Schwark et al., 1998; Hindenberg, 1999; Hammes et al., 2013; Gąsiewicz, 2013; Słowakiewicz et al., 2013, 2015) allows us to evaluate carbon burial on a basin scale. Briefly, the TOC contents of the northern margin of the SPB are low in lagoonal facies (0-0.9%, average, 0.2%), in upper slope facies (0-1.1%, average 0.2%), in oolite shoal and basinal facies (0-0.2%, average 0.1%; 0.1-1.2%, average 0.2%); they are higher in shallow-basin facies (0-1.9%, average 1.3%), and lower slope facies (0-2.1%, average 0.7%). The TOC distribution in the southern margin facies of the SPB is also variable. Specifically, the TOC contents in lower slope facies of the south-eastern SPB (SE Poland) are 0.3-2.2 wt.% (average 1.2%), whereas TOC contents in lagoonal and lower slope facies located farther westward (SE Germany) are higher (0.06-8.3%, average 1.5% and 0-2.1%, average 0.5%, respectively), and the lowest TOC content is in the oolite shoal facies (0.1-0.46%, average 0.3%). The TOC contents are considerably lower in the western SPB (NE England, lagoonal facies 0-0.2%, average 0.1%; middle slope facies 0-0.86%, average 0.2%), lower slope facies (0.0.2 %, average 0.1%) and NPB (Ettrick) (lagoonal facies 0-1.2%, average 0.3%).

The thermal maturity of north-eastern SPB (NW Poland) rocks was previously discussed in Słowakiewicz et al. (2015), whereas those from other parts of the basin have been published earlier (e.g. Schwark et al., 1998; Hindenberg, 1999; Kosakowski and Krajewski, 2014, 2015, and this study). Values obtained from vitrinite reflectance, Rock-Eval and biomarkers are broadly similar across the various parts of the SPB and NPB but generally they increase from marginal to basinal settings, although they may differ regionally according to the burial depth (e.g. Schwark et al., 1998; Hindenberg, 1999; Hartwig and Schulz, 2010; Pletsch et al., 2010; Kosakowski and Krajewski, 2014, and this study). Briefly, OM deposited in peritidal facies is immature ($R_o < 0.6$); in the ooid shoal, lagoonal and shallow basin zones it appears to be early mature (R_o 0.6-0.8); in the upper slope and lower slope facies, it is generally mature (R_o 0.8-1.0), and in basinal zones it is of variable maturity ($R_o > 0.9$). In addition, maturity of OM is lower in the north-eastern SPB than in the south-eastern SPB which could be an effect of the regional heat flow (higher in the SE SPB than in the NE SPB) (Zielinski et al., 2012).

5.2. *Indicators of redox change and depositional environment*

A suite of biomarkers was used to assess changes in water column redox potential in the NPB and SPB including the homohopane index (HHI), and the concentration of isorenieratene and chlorobactene derivatives, 28,30-bisnorhopane (BNH), and gammacerane (Table 1). Many of these parameters can also be influenced by diagenesis, source input, and thermal maturity, and these additional factors are considered in the subsequent discussion. Additional evidence for redox conditions is provided by foraminifera assemblages (Fig. 4) found in the lower slope facies.

The HHI ratio is a qualitative recorder of ancient depositional redox conditions. The C₃₅ HHI records the degree of preservation of the extended side-chain of C₃₅ hopanes derived from intact bacteriohopanepolyols (Köster et al., 1997), with high relative abundances of C₃₅ homohopanes commonly associated with marine carbonate and evaporite strata (Boon et al., 1983; Connan et al., 1986; Fu et al., 1986; ten Haven et al., 1988; Mello et al., 1988a,b; Clark and Philp, 1989) but also with the presence of reduced sulphur species (e.g., H₂S and polysulphides) in the water column (ten Haven et al., 1988; Sinninghe Damsté et al., 1995a). Unusually high concentrations of pentakishomohopanes were observed in Ca₂ sediments in the lower slope facies (well A) of the north-eastern (NE Germany) margin of the SPB, which are consistent with similar high concentrations of C₃₅ homohopanes as previously reported from the shallow basin and lower slope facies of NW Poland (NE margin of the SPB; Słowakiewicz et al., 2015) but also in hypersaline lagoonal facies of the western SPB (Table 1, Fig. 5).

In the north-eastern SPB, the lowest HHIs occur in the ooid shoal <0.1 and basinal <0.1 facies; these suggest an oxic and/or suboxic depositional environment (Fig. 6). Variable HHIs occur in the restricted lagoonal facies (HHI = 0.03-0.4), and very high HHIs occur in the shallow basin (HHI = 0.16-0.48) and lower slope (HHI = 0.05-0.49) facies, indicating an anoxic depositional environment (Fig. 6). In contrast, the southern and western margins of the SPB are characterized by more variable but low HHIs (Fig. 6): in the south-east SPB, HHIs in lower slope facies (well Gomunice-10, SE Poland) are 0.08-0.19 and decrease westward to Germany (0.08-0.09), and in the western SPB (NE England) they are 0-0.25. However, in the lagoonal facies, HHIs can be higher and are particularly variable (0.03-0.63 in S Germany and 0.04-0.28 in the western SPB) (Fig. 6). In the NPB (Ettrick), the HHIs (0-0.07) are very low.

Biomarkers for anaerobic phototrophic green sulphur bacteria provide strong constraints on the water column redox state (Summons and Powell, 1986). Isorenieratane, β -isorenieratane, C₁₅ to C₃₁ 2,3,6-aryl isoprenoids, and chlorobactane have all been found in the shallow basin and lower slope facies of the north-eastern margin of the SPB in Poland (Słowakiewicz et al., 2015), and locally in lagoons/oolite shoals of the southern SPB (SW Poland) margin (Miłow-1, depth 2004-2008 m) and lagoons of the north-eastern SPB (NW Poland) margin (KP-Z4, depth 2372-2391 m) (Fig. 6a). Variable concentrations of isorenieratane and chlorobactane (0.8 to 110 ng/g rock and 0 to 24 ng/g rock, respectively) in the NE margin shallow basin and lower slope sections have been interpreted as short-term variations during deposition of Ca₂ strata (Słowakiewicz et al., 2015). Isorenieratene derivatives have also been found in the northern margin of the SPB in NE Germany (well A). Crucially, however, they have not been detected in the southern or western SPB or the NPB sediments examined here.

28,30-bisnorhopane (BNH) is a desmethylhopane of unknown origin but it is generally regarded as indicative of anoxic to euxinic conditions in the water column (e.g. Curiale et al., 1985; Mello et al., 1990; Peters et al., 2005). BNH was detected in the lowermost lower slope and shallow basin facies in the Ca₂ on the northern margin of the eastern SPB (Słowakiewicz et al., 2015). The presence of BNH provides additional evidence that organic matter in these sedimentary settings was deposited under anoxic conditions. It was not detected in the other settings.

Although the origin of gammacerane is uncertain (Peters et al., 2005), it appears to be a diagenetic product of tetrahymanol (gammaceran-3 β -ol), a lipid that replaces steroids in ciliates feeding on bacteria at the interface between oxic and anoxic zones in stratified water columns in marine and freshwater systems (ten Haven et al., 1989; Sinninghe Damsté et al., 1995b). Gammacerane, expressed as the gammacerane index = gammacerane/(gammacerane

+ 17 α ,21 β C₃₀ hopane), was detected in the Ca2 samples from the Polish and northern and southern German part of the SPB, and in three wells (Vane Tempest VT-11, Bates Colliery B2 and Offshore Borehole-1) from the western SPB, but it was not detected in the NPB. The mean gammacerane indices are typically highest in the lagoonal facies (mean 0.19-0.5, range 0.1-0.6), high in the outer shelf, lower slope (mean 0.14-0.35, range 0.07-1) and shallow basin (mean 0.2-0.4, 0.1-0.5) facies, and not detected in the basinal facies (Fig. 6, Table 1). High gammacerane indices in the oolite (1-1.3) facies are likely due to the contact with lagoons. Due to the limited data and the relatively wide range of values that overlap among settings, gammacerane indices should be interpreted with caution. Nonetheless, on the northeast margin of the SPB, gammacerane indices are highest in the lowermost part of the lower slope and shallow basin sections, paralleling trends in BNH concentration (Słowakiewicz et al., 2015). The decoupling between high gammacerane indices and other indicators of anoxia (both temporally and among different facies) has been interpreted as recording hypersalinity and stratification rather than strictly water column redox state (Słowakiewicz et al., 2015). This would explain the high indices observed in the putatively hypersaline lagoons (NW Poland) as well as the high values in the oldest lower slope and shallow basin sediments, likely recording marine hypersalinity during the early stages of the Ca2 transgression.

5.3. Biomarker indicators of organic matter source

Compounds and compound classes can be associated with a particular biological source, such that molecular distributions can be informative about changes in the structure of the algal and microbial community. To track OM sources we examined the C₂₃ tricyclic and C₂₄ tetracyclic terpane to C₃₀ hopane ratios, various sterane and hopane ratios, and the occurrence of squalane (Table 1).

5.3.1. Terpanes

Organic matter inputs can be tentatively assessed from abundances of tricyclic and tetracyclic terpanes as well as the C_{23} tricyclic terpane/hopane (C_{23}/H) and C_{24} tetracyclic terpane/hopane (C_{24}/H) ratios; given their putative higher plant origin, they have been used as proxies for terrigenous OM inputs (Trendel et al., 1982; Aquino Neto et al., 1983; Connan et al., 1986; Noble et al., 1986). However, the source of these compounds remains elusive, and elevated concentrations of C_{24} tetracyclic terpane relative to tricyclic terpanes occur in carbonate and evaporite settings suggesting alternative origins (e.g., Connan et al., 1986; Clark and Philp, 1989; Peters et al., 2008). Moreover, the C_{23}/H ratio is strongly maturity dependent (Farrimond et al., 1999). Terpenoid ratios are significantly higher in the NPB ($C_{23}/H = 0.05$ - 1.46 , $C_{24}/H = 0.03$ - 0.8) and western SPB ($C_{23}/H = 0.01$ - 4.66 , $C_{24}/H = 0.02$ - 1.28), than in the northern ($C_{23}/H = 0.01$ - 0.46 , $C_{24}/H = 0.01$ - 0.72) and southern ($C_{23}/H = 0.06$ - 0.25 , $C_{24}/H = 0.06$ - 0.41) margins of the SPB (Fig. 6, Table 1). This could reflect relatively greater terrestrial OM inputs to the western SPB, but the aforementioned caveats dictate caution. Elemental evidence, although limited, is consistent with a greater proportion of terrigenous inputs (Gąsiewicz, 2013). Similarly, as noted in Słowakiewicz et al. (2015) and in this study, ratios are higher in basinal settings in the north-eastern SPB ($C_{23}/H = 0.14$ - 1.95 , $C_{24}/H = 0.23$ - 1) than in comparative platform settings (Fig. 6, Table 1), which could be consistent with shelf bypass and selective preservation of terrestrial OM in the former.

5.3.2. Steranes

Steranes are saturated tetracyclic compounds derived during early diagenesis from, typically, C_{27} to C_{30} sterols produced by eukaryotes. In some cases, the C_{27}/C_{29} ratio can be used to indicate the relative inputs of algae relative to higher plants based on the dominance

of C_{29} steroids in the latter (Huang and Meinschein, 1979); however, many algae also synthesize C_{29} sterols (Volkman, 1986; Volkman et al., 1998; Kodner et al., 2008) and the high C_{29} abundances could be indicative of green algal blooms (Kodner et al., 2008). The OM of the Ca2 includes abundant C_{27} - C_{29} 4-desmethyl steranes, but distributions vary markedly, both temporally and spatially, reflected in C_{27}/C_{29} ratios (Fig. 6, Table 1). The C_{27}/C_{29} sterane ratio is highest in lagoonal, oolite shoal and lower slope facies and lowest in shallow basin and basinal facies of the Ca2. It is also higher in the NPB (0.68-1.18) and western SPB (0.41-4.11), than in the northern (0.27-1.31) and southern (0.31-2.25) SPB (Fig. 6, Table 1), although Słowakiewicz et al. (2015) reported its profound temporal variability in the northeastern SPB during Ca2, distinguishing five cycles. A decoupling between C_{27}/C_{29} sterane ratios and C_{23}/H and C_{24}/H ratios suggests that low values are recording green algal inputs, especially in the northern SPB, rather than simply higher terrigenous inputs characteristic of the SPB basinal facies (Florentyna IG-2, Fig. 7).

The C_{28}/C_{29} sterane ratios in Ca2 strata (Fig. 6, Table 1) are slightly higher in the NPB (0.62-0.79) and western SPB (0.43-1.44) than in the eastern (0.27-0.94) and southern (0.26-0.84) SPB, and are generally higher (average 0.56) than the range given by Schwark and Empt (2006) for Devonian to Triassic rocks (~0.55). Building on the work of Grantham and Wakefield (1988), these workers showed a progressive increase in the C_{28}/C_{29} sterane ratio through geological time and attributed it to progressive evolution of algal communities through the Phanerozoic, possibly the replacement of more primitive C_{29} sterane-producing green-algal groups with more recent C_{28} sterane-producing red algae (Brocks and Banfield, 2009). Before the Mesozoic, however, C_{28} steranes were also likely derived from green algae, particularly prasinophytes (Kodner et al., 2008), and basin-scale trends in these ratios are harder to interpret. Others have argued (Tappan, 1980; Schwark and Empt, 2006) that high

C₂₈/C₂₉ sterane ratios could be indicative of more restricted basins; however, that interpretation is inconsistent with our observations that more restricted and reducing conditions dominated in the east. As such, it is unclear what these ratios reflect, but we attribute their variability to basin-scale differences in algal ecology.

5.3.3. Squalane

Squalane, an archaeal biomarker and a C₃₀ regular isoprenoid, has been detected in evaporitic environments, with haloarchaea and methanogenic archaea invoked as its source (Brassell et al., 1981; ten Haven et al., 1988; Vella and Holzer, 1992; Grice et al., 1998; Kluska et al., 2013). However, it could also be a diagenetic product of squalene which occurs in many organisms. Squalane was detected in Ca₂ transgressive stromatolites of Offshore Borehole-1 (Fig. 5); the microorganisms forming those structures likely used Hartlepool Anhydrite (A1) sulphates of the Zechstein first cycle (Z1) as a substrate, such that the presence of squalane is partially related to a local evaporitic environment.

6. Discussion

6.1. Sources of OM and implications for productivity

Algal-, bacterial- and terrestrial- derived biomarker distributions confirm the variety of OM sources in both the SPB and NPB basins. Specifically, OM in the western SPB could have significant terrestrial component which is proportionally higher than in the NPB and southern and northern-eastern SPB. This is suggested by high terpenoid ratios (average C₂₃/H = 1.85, C₂₄/H = 0.53), but also supported fossilized plants in Ca₂ deposits (Schweitzer, 1986; Uhl, 2004). Consistent with Słowakiewicz et al. (2015), basin sediments also appear to be dominated by a greater proportion of terrestrial relative to marine organic matter (Florentyna IG-2, Piła IG-1, Figs 6,7), which we have argued is mostly due to enhanced preservation of terrestrial relative to marine OM under oxidising conditions (Słowakiewicz et al., 2015). OM

in the southern and northern margins of the SPB is predominantly represented by an algal-bacterial type of OM, although co-occurring with significant terrestrial (liptinite) OM component (black laminae in lower slope facies, Fig. 8a-b). A bacterial and algal (lamalginite) component of OM is likely important in various intertidal microbialites in more restricted and hypersaline lagoons of the SPB (Fig. 8c-e).

OM sources in the Ca2 SPB sections are also characterised by profound temporal variability expressed by C_{27}/C_{29} and C_{28}/C_{29} sterane ratios in the lagoonal and lower slope facies (Fig. 7). Słowakiewicz et al. (2015) observed similar dramatic variations in C_{27}/C_{29} (short-term five cycles) and C_{28}/C_{29} sterane ratios in the lower slope facies, which were interpreted as recording changes in the algal assemblage rather than marine vs. terrestrial inputs; although our basin-scale data is not of comparable resolution, it also reveals pronounced temporal variability. We suggest that these variations are the result of orbital forcing (Słowakiewicz et al., 2015), which amongst other things can control the productivity of organic carbon, as has been demonstrated for the Jurassic Kimmeridge Clay Formation (Weedon et al., 2004), Mesozoic oceanic anoxic events (e.g. Hofmann et al., 2003; Kuypers et al., 2004a,b; Li et al., 2008; Blumenberg and Wiese, 2012), and the Pliocene–Pleistocene sapropels in the Mediterranean area (Lourens et al., 1996; Roveri and Taviani, 2003). Orbital forcing likely brought about changes in nutrient inputs causing changes in algal ecology as expressed by C_{27}/C_{29} and C_{28}/C_{29} sterane ratios and increased productivity in the eastern SPB. Similar variations have also been observed in isorenieratane and chlorobactane concentrations, reflecting periodic expansion of PZE driven by increased productivity (Słowakiewicz et al., 2015).

Sterane distributions also suggest basin-scale variations in algal assemblages. High C_{27}/C_{29} sterane ratios in the western SPB suggest that marine productivity there was partially

governed by green algal blooms. However, C₂₈/C₂₉ sterane ratios are also high in the eastern SPB and that is difficult to interpret. Nonetheless, it is likely that the strong spatial and temporal variations of algal assemblages in the SPB were dictated by environmental conditions some of which may have been controlled by orbital forcing.

Therefore, OM accumulation in the SPB is governed by a complex range of controls such as sedimentation rate, grain-size, anaerobic respiration, productivity and oxic/anoxic cycles, giving rise to highly spatially and temporally heterogeneous TOC contents. TOC contents are the highest in oxic-anoxic restricted lagoons of the southern SPB. They are moderately high on the euxinic northern and oxygen-depleted south-east corner of the SPB – but even in these areas, TOC contents are highly variable. Temporal variability of redox conditions is also evidenced from the presence of a benthic fauna and bioturbation, indicating that oxic-anoxia fluctuated throughout deposition of the Ca₂ sediments. Certainly, and as described in the next section, a simple model of basin-scale stratification, anoxia and OM accumulation is inappropriate.

6.2. Distribution of anoxia

Using a GENIE Earth system model, Meyer et al. (2008) demonstrated that Late Permian seas and oceans varied significantly in their biogeochemistry. The upper portion of the world-spanning Panthalassa water column remained well oxygenated with dysoxic (0.2 – 2.0 ml O₂ L⁻¹) bottom waters, whereas the Palaeo-Tethys Ocean was largely sulphidic, and the Neo-Tethys Ocean and the Boreal Sea had oxic waters. Questions, however, have arisen as to whether the Boreal Sea was truly oxic. For example, biomarker (Hays et al., 2012), $\delta^{114/110}\text{Cd}$ (Georgiev et al., 2015), and framboidal pyrite data (Nielsen and Shen, 2004) strongly suggest a sulphidic or at least partly sulphidic water column in the Boreal Sea, which was connected with the NPB of Europe. The contradictory results confirm that partially restricted basins can

be difficult to model and that sedimentological and geochemical tools are essential to reconstruct their biogeochemical conditions.

Similarly, contradictory sedimentary, fossil and geochemical data suggest that deposition in the SPB during Ca2 was also complex. As noted above, in some slope facies biomarkers for GSB and high HHIs indicate anoxic conditions that occasionally extended into the photic zone. However, fragments of thin-shelled bivalves, ostracods, calcispheres, nodosarid foraminifera, millimetre-scale burrows (Słowakiewicz et al., 2015), and rare bryozoans (Hara et al., 2009), also occur in the Ca2 lagoonal and slope facies. Specifically, nodosarid foraminifera seem to be most common within lower slope facies (wells: B and WK-8; Fig. 4) of the SPB northern margin, but *Ammodiscus*, *Glomospira*, *Calcitornella*, *Lingulina*, *Lunucamina*, and *Tolypammia* foraminifera have also been reported from the Ca2 facies (Peryt and Woszczyńska, 2001). The nodosarid foraminifera found in the slope facies are a benthic foraminifera likely to have been tolerant of suboxic (0.3-1.6 mL/L O₂) conditions (Kaiho, 1994) but probably not anoxic conditions. In total, the combination of biomarker and benthic faunal proxies indicates that on the northern margin of the SPB, organic matter in the lower slope and shallow-basin facies was deposited under fluctuating but frequently anoxic conditions; moreover isorenieratane and chlorobactane indicate that euxinia extended into the photic zone of the water column, at least from well Czarne-2 in the east to well A in the western part of the northern margin (Fig. 9).

However, our new data expands on and confirms the observation of Słowakiewicz et al. (2015) that this intermittent water column anoxia was limited to the north-eastern platform (including lower slope and shallow-basin facies) of the SPB. The absence of 28,30-bisnorhopane and isorenieratane (and its derivatives) in samples from basinal and outer ooid-shoal facies, and low HHIs (and low TOC contents), all suggest that suboxic conditions

occurred on the basin-floor of the periodically refreshed eastern SPB (Fig. 9). This interpretation is confirmed by new data from basinal settings in the southern and western SPB, confirming that anoxia did not develop basin-wide (Fig. 9).

The southern margin of the basin also appears to have been well oxygenated (well C, HHI = 0.08-0.09; no evidence of isorenieratene derivatives, Fig. 7). Schwark et al. (1998) reported higher HHIs (0.17-0.26) from slope facies of Sprötau Z1 and interpreted the accumulation of OM as favoured by reducing conditions. However, Sprötau Z1 was drilled in a small embayment/shallow basin (Fig. 1b) where more reducing conditions naturally would be expected. Therefore, we instead interpret these results as a local manifestation of anoxic conditions. Fluctuating oxic-euxinic-anoxic conditions also occurred in restricted lagoons of the southern margin (HHI = 0.03-0.4).

Moreover, evidence for anoxic conditions in the western and central SPB (south-central lagoons, Slach, 1993; Hofmann and Leythaeuser, 1995) is lacking and it is suggested that deposition of OM in these portions of the SPB was essentially under oxic-suboxic marine conditions (as presented in the depositional models of the Ca₂ shown in Figs 9,10). Our data also do not support anoxic conditions in the NPB. We suggest that anoxia did not occur in the less restricted NPB because water in the NPB and SPB came from Panthalassa Ocean via a relatively oxic Boreal Sea. As noted earlier, the occurrence of an essentially oxygenated upper portion of the Panthalassa water column and oxic Boreal Sea in the Late Permian is also suggested by GENIE simulations (Meyer et al., 2008). Of course, more reducing and even euxinic conditions likely existed in restricted lagoons dominated by production of microbialites under high salinity conditions (Słowakiewicz et al., 2015 and this study). Nor can we preclude the possibility of some deep anoxic water in lows on the deep basin floor in the centre of the SPB too.

Nonetheless, the collective evidence clearly indicates that anoxia was not persistent at the basin scale but was restricted to nearshore settings of the north-eastern SPB. It also shows the spatial variety of redox conditions in the SPB, from more oxic in the west to more anoxic in the east (Fig. 11). It has been argued that the Messinian and Pliocene-Pleistocene sapropel model of deposition (e.g. Emeis et al., 2000; Liu et al., 2012; Taylforth et al., 2014), is applicable to the epeiric NPB and SPB (Turner and Magaritz, 1986; Pancost et al., 2002; McCann et al., 2008; Peryt et al., 2010), whereby anoxic/euxinic conditions in a deep basin resulted from freshwater input into a relatively restricted basin which brought about a density stratification, and, if associated with increased nutrient inputs, stimulated productivity (Emeis et al., 2000). However, our results indicate that this model, as well as the Black Sea (Arthur and Sageman, 1994) and bath-tub ring (Frakes and Bolton, 1984; Wignall and Newton, 2001) models, are inappropriate for the NPB and SPB during the Ca2 interval. PZE, which is typically associated with a stratified water column (Kenig et al., 2004; Wagner et al., 2004), was largely restricted to the north-eastern SPB margin and did not extend into the wider basin (Fig. 11).

It is generally accepted that in early Zechstein time the SPB was fed by open-ocean waters coming through the relatively narrow Norwegian-Greenland strait to the north (Taylor, 1998; Legler and Schneider, 2008). However, other routes for Zechstein flooding of the SPB have been suggested, e.g., the flooding may have also occurred around or across the Pennines from the Irish (Bakevellia) Sea, via the Fair Isle and Moray Firth basins (Smith and Taylor, 1992), or via a temporary connection to the SE with the Palaeo-Tethys Ocean (Peryt and Peryt, 1977; Ziegler et al., 1997; Şengör and Atayman, 2009, Fig. 1a).

The possibility of at least a periodic SE connection also seems to be supported by the biomarker distribution from well Gomunice-10 (Fig. 7). The Gomunice section (Ca2 = 31.3 m thick) is represented by mainly non-laminated dolomitic mudstone with bioclastic

wackestone in the lowermost part (marking the transgression of the Ca2 sea, Fig. 7). Isorenieratene and chlorobactene derivatives, gammacerane and BNH were not detected in any of the 12 samples from this well, suggesting a lack of elevated salinity as well as no euxinic or anoxic conditions. The HHI is rather low (0.08-0.19) in the whole section and slightly decreases from 0.13 to 0.08 up section (HHI is the highest [0.3] in the uppermost part, close to the contact with the overlying Basal Anhydrite [A2]), suggesting progressive oxygen enrichment in the water column (Fig. 7). The increasing up-section trend, however, is observed in the C₂₇/C₂₉ and C₂₈/C₂₉ sterane ratios, unlike in the SPB northeastern margin where they have a fluctuating pattern (Fig. 7). If the south-east connection with the Palaeo-Tethys Ocean existed it could have prevented restricted marine conditions in this area as a result of seawater exchange and explain why biomarker indices for anoxia differ so markedly between these two areas.

We also suggest that anoxia during the Ca2 cycle was driven by more local or regional processes, such as elevated productivity, sedimentation rate, grain size and anaerobic respiration. Key to this interpretation is the observation that even in the lower slope facies of the NE SPB, highly variable TOC contents (0-2.1%, average 0.7% on lower slope, 0-1.9%, average 1.3% in the shallow basin) (Słowakiewicz et al., 2013, and this study), isorenieratene derivative concentrations, and sterane ratios imply a very dynamic oxic-anoxic environment, with the cycles in biomarker distributions reported by Słowakiewicz et al. (2015) potentially being orbitally modulated. Moreover, isorenieratane often occurs in bioturbated sediments containing a benthic fauna, suggesting periodic alternation of euxinic and oxic-suboxic water-column conditions, similar to that suggested for the Oxford Clay Formation in south-central England in which isorenieratane and a benthic fauna also co-occur (Kenig et al., 2004). Therefore, OM productivity and preservation could have been governed by the range of temporally dynamic processes mentioned above.

The combination of localised anoxia that is highly temporally variable is consistent with a model in which productivity variations are modulated by hydrological changes in nutrient discharge, as is increasingly invoked for Mesozoic OAEs (Blättler et al., 2011; Monteiro et al., 2012; Pogge von Strandmann et al., 2013). A productivity explanation is consistent with a green algal bloom origin for relatively high C₂₉ sterane abundances in the north-eastern part of the SPB. It is also consistent with $\delta^{13}\text{C}$ data from the carbonate sediments deposited in the NPB and SPB (Słowakiewicz et al., 2015 and Table 2) which suggest increased productivity through the Ca2 (Słowakiewicz et al., 2015). The essentially more ramp-like morphology of the northern platform slopes in the Polish sub-basin could also have fostered relatively higher primary productivity via enhanced nutrient transport from the platform interior, whereas in the case of the largely steep, high-angle southern margins OM mostly accumulated in the toe-of-slope zones. Therefore, anoxia is not a basin-scale phenomenon as has been previously inferred but is a highly localised feature, perhaps facilitated by basin geometry, continental processes and/or regional oceanography, all contributing to high primary organic matter productivity.

Collectively, our data challenge extrapolation of observations from marginal settings to characterize wider basin environmental conditions, especially when those observations are only directly recording local conditions, i.e. overlying water column redox state. Therefore, caution should be exercised in the extrapolation of evidence for PZE when it is geographically restricted. This is the case for many investigations of, for example, PZE at the Permian/Triassic boundary (e.g., Grice et al., 2005; Cao et al., 2009; Hays et al., 2012), the Frasnian/Famnenian boundary (Joachimski et al., 2001; Bond et al., 2004) and the Triassic/Jurassic boundary (Hesselbo et al., 2007; Williford et al., 2014). Those studies remain vital contributions to the understanding of those time intervals but they illustrate the

difficulty of reconstructing wide-scale oceanographic conditions when available deposits are limited to marginal settings. Instead, interpretation should be based on either datasets with a relatively wide geographic coverage or complemented by the use of alternative proxies that record more widespread basin-scale changes in seawater chemistry (e.g. Schobben et al., 2015).

Conclusions

Biomarker, carbon and oxygen isotopic, and palaeontological data from the NPB and SPB, where the Ca₂ was deposited in a shallow- to deep- marine setting, suggest that euxinia periodically impinged on the lower slope and in the shallow basin of the SPB northern margin. Redox-sensitive biomarkers such as bisnorhopane, chlorobactane and isorenieratane (and its derivatives) are present in samples from shallow-basin and lower slope facies in the north-eastern SPB; isorenieratene derivatives are localised in more restricted lagoons of the NE SPB and SE SPB. The absence of bisnorhopane and isorenieratene derivatives in other facies of the NPB and SPB, and with homohopane indices frequently below 0.1, suggest oxic to suboxic bottom waters. More specifically, the NPB with its connection to the Boreal Sea had a normal salinity oxic water column with normal salinity seawater input from the Panthalassa Ocean and the Boreal Sea. The western SPB was characterized by slightly elevated salinity, stratification and an oxic-suboxic water column with oxic seawater input from the Boreal Sea. The southern SPB was likely characterized by more reducing conditions developed in embayments with elevated salinity (restricted lagoons) and a stratified water column. In contrast to all of these, the north-eastern SPB was characterised by periodic PZE and anoxic depositional conditions. Crucially, the restriction of PZE to only the northern margin of the SPB argues against stratification of the Ca₂ basin, wherein anoxia at other nearshore settings would be expected (i.e. the bath-tub ring model, Frakes and Bolton, 1984;

Wignall and Newton, 2001). Instead, reducing conditions in this area appear to be due to a combination of more localised phenomena, including slope topography and local climatic controls.

Acknowledgements

British Geological Survey (Keyworth) and Polish Geological Institute (Warsaw) are thanked for permission to access the core stores. We would like to thank Ian Boomer (Birmingham University) for performing carbon and oxygen analyses. We also wish to thank NERC for partial funding of the mass spectrometry facilities at Bristol (contract no. R8/H10/63). We appreciate the helpful comments of David Bottjer and an anonymous reviewer to improve our manuscript. MS was supported by a Mobility Plus programme post-doctoral fellowship from the Ministry of Science and Higher Education, Poland and Shell Exploration & Production. RDP acknowledges the Royal Society Wolfson Research Merit Award.

References

- Aquino Neto, F.R., Trendel, J.M., Restle, A., Connan, J., Albrecht, P.A., 1983. Occurrence and formation of tricyclic and tetracyclic terpanes in sediments and petroleums. In: Bjorøy, M., Albrecht, K., Cornford, K., de Groot, G., Eglinton, G., Galimov, E., Leythaeuser, D., Pelet, R., Rullkötter, J., Speers, G. (Eds.), *Advances in Organic Geochemistry 1981*. John Wiley & Sons, New York, pp. 659-676.
- Arthur, M.A., Sageman, B.B., 1994. Marine black shales: depositional mechanisms and environments of ancient deposits. *Annual Review of Earth and Planetary Sciences* 22, 499-551.
- Bergamaschi, B.A., Tsamakis, E., Keil, R.G., Eglinton, T.I., Montluçon, D.B., Hedges, J.I., 1997. The effect of grain size and surface area on organic matter, lignin and carbohydrate concentrations and molecular compositions in Peru Margin sediments. *Geochimica et Cosmochimica Acta* 61, 1247-1260.

646 Blättler, C.L., Jenkyns, H.C., Reynard, L.M., Henderson, G.M., 2011. Significant increases in global
647 weathering during Oceanic Anoxic Events 1a and 2 indicated by calcium isotopes. *Earth and*
648 *Planetary Science Letters* 309, 77-88.

649 Blakey, R., 2015. European Paleogeographic Maps. <http://cpgeosystems.com/euromaps.html>

650 Blumenberg, M., Wiese, F., 2012. Imbalanced nutrients as triggers for black shale formation in a
651 shallow shelf setting during the OAE 2 (Wunstorf, Germany). *Biogeosciences* 9, 4139-4153.

652 Bond, D., Wignall, P.B., Racki, G., 2004. Extent and duration of marine anoxia during the Frasnian-
653 Famennian (Late Devonian) mass extinction in Poland, Germany, Austria and France. *Geological*
654 *Magazine* 141, 173-193.

655 Boon, J.J., Hine, S.H., Burlingame, A.L., Klok, J., Rijpstra, W.I.C., de Leeuw, J.W., Edmunds, K.E.,
656 Eglinton, G., 1983. Organic geochemical studies of Solar Lake laminated cyanobacterial mats. In:
657 Bjørøy, M., Albrecht, K., Cornford, K., de Groot, G., Eglinton, G., Galimov, E., Leythaeuser, D.,
658 Pelet, R., Rullkötter, J., Speers, G. (Eds.), *Advances in Organic Geochemistry 1981*. John Wiley &
659 Sons, New York, pp. 207-227.

660

661 Brassell, S.C., Wardroper, A.M.K., Thomson, I.D., Maxwell, J.R., Eglinton, G., 1981. Specific
662 acyclic isoprenoids as biological markers of methanogenic bacteria in marine sediments. *Nature* 290,
663 693-696.

664

665 Brocks, J.J., Banfield, J., 2009. Unravelling ancient microbial history with community
666 proteogenomics and lipid geochemistry. *Nature Reviews Microbiology* 7, 601-609.

667 Brongersma-Sanders, M., 1971. Origin of major cyclicity of evaporites and bituminous rocks: an
668 actualistic model. *Marine Geology* 11, 123-144.

669 Cao, C., Love, G.D., Hays, L.E., Wang, W., Shen, S., Summons, R.E., 2009. Biogeochemical
670 evidence for euxinic oceans and ecological disturbance presaging the end-Permian mass extinction
671 event. *Earth and Planetary Science Letters* 281, 188-201.

672 Canfield, D.E., 1994. Factors influencing organic carbon preservation in marine sediments. *Chemical*
673 *Geology* 114, 315-329.

674 Canfield, D.E., Kristensen, E., Thamdrup, B., 2005. The oxygen cycle. In: Canfield, D.E., Kristensen,
675 E., Thamdrup, B. (eds), *Aquatic Geomicrobiology. Advances in Marine Biology* 48, 167–204.

676 Clark, J.P., Philp, R.P., 1989. Geochemical characterization of evaporite and carbonate depositional
677 environments and correlation of associated crude oils in the Black Creek Basin, Alberta. *Canadian*
678 *Petroleum Geologists Bulletin* 37, 401-416.

679

680 Connan, J., Bouroullec, J., Dessort, D., Albrecht, P., 1986. The microbial input in carbonate-anhydrite
681 facies of a sabkha palaeoenvironment from Guatemala: a molecular approach. *Organic Geochemistry*
682 10, 29-50.

683 Curiale, J.A., Cameron, D., Davis, D.V., 1985. Biological marker distribution and significance in oils
684 and rocks of the Monterey Formation, California. *Geochimica et Cosmochimica Acta* 49, 271-288.

685 Ducklow, H.W., Steinberg, D.K., 2001. Upper ocean carbon export and the biological pump.
686 *Oceanography* 14, 50-58.

687

688 Emeis, K.-C., Sakamoto, T., Wehausen, R., Brumsack, H.-J., 2000. The sapropel record of the eastern
689 Mediterranean Sea – results of Ocean Drilling Program Leg 160. *Palaeogeography, Palaeoclimatology,*
690 *Palaeoecology* 158, 371-395.

691

692 Farrimond, P., Bevan, J.C., Bishop, A.N., 1999. Tricyclic terpane maturity parameters: response to
693 heating by an igneous intrusion. *Organic Geochemistry* 30, 1011-1019.

694 Frakes, L.A., Bolton, B.R., 1984. Origin of manganese giants: sea-level change and anoxic-oxic
695 history. *Geology* 12, 83-86.

696

697 Fu, J., Sheng, G., Peng, P., Brassell, S.C., Eglinton, G., Jigang, J., 1986. Peculiarities of salt lake
698 sediments as potential source rocks in China. *Organic Geochemistry* 10, 119-126.

699

700 Gast, R., 1988. Rifting im Rotliegenden Niedersachsens. *Die Geowissenschaften*, 6, 115-122.

701 Gąsiewicz, A., 2013. Climatic control on the Late Permian Main Dolomite (Ca₂) deposition in
702 northern margin of the Southern Permian Basin and implications to its internal cyclicity. In:
703 Gąsiewicz, A., Słowakiewicz, M. (Eds.), *Palaeozoic Climate Cycles: Their Evolutionary and*
704 *Sedimentological Impact*. Geological Society, London, Special Publications 376, 475-521.

705

706 Georgiev, S.V., Horner, T.J., Stein, H.J., Hannah, J.L., Bingen, B., Rehkämper, M., 2015. Cadmium-
707 isotopic evidence for increasing primary productivity during the Late Permian anoxic event. *Earth and*
708 *Planetary Science Letters* 410, 84-96.

709 Gibbison, R., Peakman, T.M., Maxwell, J.R., 1995. Novel porphyrins as molecular fossils for
710 anoxygenic photosynthesis. *Tetrahedron Letters* 36, 9057-9060.

711 Glennie, K.W., 1998. Lower Permian-Rotliegend. In: Glennie, K.W. (ed.) *Petroleum Geology of the*
712 *North Sea*. Blackwell Scientific Publications, Oxford, 137-174.

713 Glennie, K.W., Higham, J., Stemmerik, L., 2003. Permian. In: Evans, D., Grahan, C., Armour, R.,
714 Bathurst, P. (eds.) *The Millennium Atlas: Petroleum Geology of the Central and Northern North Sea*.
715 Geological Society, London, 91-103.

716 Grantham, P.J., Wakefield, L.L., 1988. Variations in the sterane carbon number distributions of
717 marine source rock derived crude oils through geological times. *Organic Geochemistry* 12, 61-77.

718 Grice, K., Schaeffer, P., Schwark, L., Maxwell, J.R., 1996a. Molecular indicators of
719 palaeoenvironmental conditions in an immature Permian shale (Kupferschiefer, Lower Rhine Basin,
720 north-west Germany) from free and S-bound lipids. *Organic Geochemistry* 25, 131-147.

721 Grice, K., Gibbison, R., Atkinson, J.E., Schwark, L., Eckardt, C.B., Maxwell, J.R., 1996b.
722 Maleimides (1*H*-pyrrole-2,5-diones) as molecular indicators of anoxygenic photosynthesis in ancient
723 water columns. *Geochimica et Cosmochimica Acta* 60, 3913-3924.

724 Grice, K., Schaeffer, P., Schwark, L., Maxwell, J.R., 1997. Changes in palaeoenvironmental condition
 725 during deposition of the Permian Kupferschiefer (Lower Rhine Basin, northwest Germany) inferred
 726 from molecular and isotopic compositions of biomarker components. *Organic Geochemistry* 26, 677-
 727 690.

728 Grice, K., Schouten, S., Nissenbaum, A., Charrach, J., Sinninghe Damsté, J.S., 1998. Isotopically
 729 heavy carbon in the C₂₁ to C₂₅ regular isoprenoids in halite-rich deposits from the Sdom Formation,
 730 Dead Sea Basin, Israel. *Organic Geochemistry* 28, 349-359.

731 Grice, K., Cao, C.Q., Love, G.D., Böttcher, M.E., Twitchett, R.J., Grosjean, E., Summons, R.E.,
 732 Turgeon, S.C., Dunning, W., Jin, Y.G., 2005. Photic zone euxinia during the Permian-Triassic
 733 superanoxic event. *Science* 307, 706-709.

734

735 Grotzinger, J.P., Knoll, A.H., 1995. Anomalous carbonate precipitates: Is the Precambrian the key to
 736 the Permian? *Palaios* 10, 578-596.

737

738 Hain, M.P., Sigman, D.M., Haug, G.H., 2014. The biological pump in the past. In: Holland, H.D.,
 739 Turekian, K.K. (Eds.), *Treatise in Geochemistry*. 2nd ed. Elsevier, Oxford, pp. 485-517.

740

741 Hammes, U., Krause, M., Mutti, M., 2013. Unconventional reservoir potential of the upper Permian
 742 Zechstein Group: a slope to basin sequence stratigraphic and sedimentological evaluation of
 743 carbonates and organic-rich mudrocks, Northern Germany. *Environmental Earth Sciences*, 70, 3797-
 744 3816.

745

746 Hara, U., Ernst, A., Mikołajewski, Z., 2009. Permian trepostome bryozoans from the Zechstein Main
 747 Dolomite (Ca₂) of western Poland and NE Germany. *Geological Quarterly* 53, 249-254.

748 Hartwig, A., Schulz, H.-M., 2010. Applying classical shale gas evaluation concepts to Germany – Part
 749 I: The basin and slope deposits of the Stassfurt Carbonate (Ca₂, Zechstein, Upper Permian) in
 750 Brandenburg. *Chemie der Erde* 70, 77-91.

751 Hedges, J.I., Keil, R.G., 1995. Sedimentary organic matter preservation: an assessment and
752 speculative synthesis. *Marine Chemistry* 49, 81-115.

753 Henrichs, S. M., 1992. The early diagenesis of organic matter in marine sediments: Progress and
754 perplexity. *Marine Chemistry* 39, 119–149.

755 Hesselbo, S.P., McRoberts, C.A., Pálffy, J., 2007. Triassic-Jurassic boundary events: problems,
756 progress, possibilities. *Palaeogeography, Palaeoclimatology, Palaeoecology* 244, 1-10.

757 Hays, L.E., Grice, K., Foster, C.B., Summons, R.E., 2012. Biomarker and isotopic trends in a
758 Permian-Triassic sedimentary section at Kap Stosch, Greenland. *Organic Geochemistry* 43, 67-82.

759

760 Henderson, C.M., Mei, S., 2000. Geographical cline in Permian neogondolellids and its role in
761 taxonomy: A brief introduction. *Permophiles*, 36, 32-37.

762

763 Hendry, J.P., Kalin, R.M., 1997. Are oxygen and carbon isotopes of mollusc shells reliable
764 palaeosalinity indicators in marginal marine environments? A case study from the Middle Jurassic of
765 England. *Journal of the Geological Society, London*, 154, 321–333.

766 Hindenberg, K., 1999. Genese, Migration und Akkumulation von Erdöl in Mutter- und
767 Speichergesteinen des Staßfurt-Karbonat (Ca₂) von Mecklenburg-Vorpommern und Südost-
768 Brandenburg. PhD thesis, University of Jülich, 3698, 185pp.

769 Hofmann, P., Leythaeuser, D., 1995. Migration of hydrocarbons in carbonate source rocks of the
770 Staßfurt member (Ca₂) of the Permian Zechstein, borehole Aue 1, Germany: the role of solution
771 seams. *Organic Geochemistry* 23, 597-606.

772 Hofmann, P., Wagner, T., Beckmann, B., 2003. Millennial- to centennial-scale record of African
773 climate variability and organic carbon accumulation in the Coniacian–Santonian eastern tropical
774 Atlantic (Ocean Drilling Program Site 959, off Ivory Coast and Ghana). *Geology* 31, 135–138.

775 Huang, W.-Y., Meinschein, W.G., 1979. Sterols as ecological indicators. *Geochimica et*
776 *Cosmochimica Acta* 43, 739-745.

777 Jenkyns, H.C., 1985. The Early Toarcian and Cenomanian-Turonian anoxic events in Europe:
778 comparisons and contrasts. *Geologische Rundschau* 74/3, 505-518.
779

780 Jenkyns, H.C., 1988. The Early Toarcian (Jurassic) anoxic event: Stratigraphic, sedimentary, and
781 geochemical evidence. *American Journal of Science* 288, 101-151.

782 Jenkyns, H.C. 2010. Geochemistry of ocean anoxic events. *Geochemistry Geophysics Geosystems*, 11,
783 Q03004, doi:10.1029/2009GC002788

784 Joachimski, M.M., Ostertag-Henning, C., Pancost, R.D., Strauss, H., Freeman, K.H., Littke, R.,
785 Sinninghe Damsté, J.S., Racki, G., 2001. Water column anoxia, enhanced productivity and
786 concomitant changes in $\delta^{13}\text{C}$ and $\delta^{34}\text{S}$ across the Frasnian-Famennian boundary (Kowala – Holy Cross
787 Mountains/Poland). *Chemical Geology* 175, 109-131.

788 Kaiho, K., 1994. Benthic foraminiferal dissolved-oxygen index and dissolved-oxygen levels in the
789 modern ocean. *Geology* 22, 719-722.

790 Kenig, F., Hudson, J.D., Sinninghe Damsté, J.S., Popp, B.N., 2004. Intermittent euxinia:
791 Reconciliation of a Jurassic black shale with its biofacies. *Geology* 32, 421-424.

792 Khiel, J.T., Shields, C.A., 2005. Climate simulation of the latest Permian: Implications for mass
793 extinction. *Geology* 33, 757-760.

794 Kiersnowski, H., Paul, J., Peryt, T.M., Smith, D., 1995. Facies, palaeogeography and sedimentary
795 history of the Southern Permian Basin in Europe. In: Scholle, P., Peryt, T.M., Ulmer-Scholle, D.S.
796 (eds) *The Permian of Northern Pangea*. Springer-Verlag, Berlin, 2, 119-136.

797 Kluska, B., Rospondek, M.J., Marynowski, L., Schaeffer, P., 2013. The Werra cyclotheme (Upper
798 Permian, Fore-Sudetic Monocline, Poland): Insights into fluctuations of the sedimentary environment
799 from organic geochemical studies. *Applied Geochemistry* 29, 73-91.

800 Kodner, R.B., Pearson, A., Summons, R.E., Knoll, A.H., 2008. Sterols in red and green algae:
801 quantification, phylogeny, and relevance for the interpretation of geologic steranes. *Geobiology* 6,
802 411-420.

803 Kosakowski, P., Krajewski, M., 2014. Hydrocarbon potential of the Zechstein Main Dolomite in the
804 western part of the Wielkopolska platform, SW Poland: New sedimentological and geochemical data.
805 *Marine and Petroleum Geology* 49, 99-120.

806 Kosakowski, P., Krajewski, M., 2015. Hydrocarbon potential of the Zechstein Main Dolomite (Upper
807 Permian) in western Poland: relation to organic matter and facies characteristics. *Marine and*
808 *Petroleum Geology* 68, 675-694.

809 Köster, J., van Kaam-Peters, H., Koopmans, M., de Leeuw, J., Sinninghe Damsté, J., 1997.
810 Sulphurisation of homohopaneoids: Effects on carbon number distribution, speciation, and 22S/22R
811 epimer ratios. *Geochimica et Cosmochimica Acta* 61, 2431-2452.

812 Kuypers, M.M.M., Pancost, R.D., Nijenhuis, I.A., Sinninghe Damsté, J.S., 2002. Enhanced
813 productivity led to increased organic carbon burial in the euxinic North Atlantic basin during the late
814 Cenomanian oceanic anoxic event. *Paleoceanography* 17, 1051.

815

816 Kuypers, M.M.M., Lourens, L.J., Rijpstra, W.I.C., Pancost, R.D., Nijenhuis, I.A., Sinninghe Damsté,
817 J.S., 2004a. Orbital forcing of organic carbon burial in the proto-North Atlantic during oceanic anoxic
818 event 2. *Earth and Planetary Science Letters* 228, 465-482.

819 Kuypers, M.M.M., van Breugel, Y., Schouten, S., Erba, E., Sinninghe Damsté, J.S., 2004b. N₂-fixing
820 cyanobacteria supplied nutrient N for Cretaceous oceanic anoxic events. *Geology* 32, 853-856.

821

822 Lazar, B., Erez, J., 1990. Extreme ¹³C depletions in seawater-derived brines and their implications for
823 the past geochemical carbon cycle. *Geology* 18, 1191-1194.

824

825 Legler, B., Schneider, J.W., 2008. Marine ingressions into the Middle/Late Permian saline lake of the
826 Southern Permian Basin (Rotliegend, Northern Germany) possibly linked to sea-level highstands in
827 the Arctic rift. *Palaeogeography, Palaeoclimatology, Palaeoecology*, 267, 102-114.

828 Li, Y.-X., Bralower, T.J., Montañez, I.P., Osleger, D.A., Arthur, M.A., Bice, D.M., Herbert, T.D.,
829 Erba, E., Silva, I.P., 2008. Toward an orbital chronology for the early Aptian Oceanic Anoxic Event
830 (OAE1a, ~120 Ma). *Earth and Planetary Science Letters* 271, 88-100.

831

832 Liu, Q., Larrasoana, Torrent, J., Roberts, A.P., Rohling, E.J., Liu, Z., Jiang, Z., 2012. New constraints
833 on climate forcing and variability in the circum-Mediterranean region from magnetic and geochemical
834 observations of sapropels S1, S5 and S6. *Palaeogeography, Palaeoclimatology, Palaeoecology* 333-
835 334, 1-12.

836 Lourens, L.J., Hilgen, F.J., Zachariase, W.J., van Hoof, A.A.M., Antonarakou, A., Vergnaud-Grazzini,
837 C., 1996. Evaluation of the Pliocene to early Pleistocene astronomical time scale. *Palaeoceanography*
838 11, 391-413.

839 Mayer, L.M., 1994. Relationships between mineral surfaces and organic carbon concentrations in
840 soils and sediments. *Chemical Geology* 114, 347-363.

841 Mayer, L.M., 1995. Sedimentary organic matter preservation: an assessment and speculative synthesis
842 – a comment. *Marine Chemistry* 49, 123-126.

843 McCann, T., Kiersnowski, H., Krainer, K., Vozárová, A., Peryt, T.M., Oplustil, S., Stollhofen, H.,
844 Schneider, J., Wetzel, A., Boulvain, F., Dusa, M., Török, Á., Haas, J., Tait, J., Körner, F., 2008.
845 Permian. In: McCann, T. (Ed.), *The Geology of Central Europe. Volume 1: Precambrian and*
846 *Palaeozoic*. The Geological Society, London, 531-597.

847

848 Mello, M.R., Gaglianone, P.C., Brassell, S.C., Maxwell, J.R., 1988a. Geochemical and biological
849 marker assessment of depositional environments using Brazilian offshore oils. *Marine and Petroleum*
850 *Geology* 5, 205-223.

851

852 Mello, M.R., Telnaes, N., Gaglianone, P.C., 1988b. Organic geochemical characterization of
853 depositional paleoenvironments in Brazilian marginal basin. *Organic Geochemistry* 13, 31-46.

854

855 Mello, M.R., Koutsoukos, E.A.M., Hart, M.B., Brassell, S.C., Maxwell, J.R., 1990. Late Cretaceous
856 anoxic events in the Brazilian continental margin. *Organic Geochemistry* 14, 529-542.

857

858 Meyer, K.M., Kump, L.R., Ridgwell, R., 2008. Biogeochemical controls on photic-zone euxinia
859 during the end-Permian mass extinction. *Geology* 36, 747-750.

860

861 Monteiro, F.M., Pancost, R.D., Ridgwell, A., Donnadieu, Y., 2012. Nutrients as the dominant control
862 on the spread of anoxia and euxinia across the Cenomanian-Turonian oceanic anoxic event (OAE2):
863 model-data comparison. *Paleoceanography* 27, PA4209.

864

865 Müller, P.J., Suess, E., 1979. Productivity, sedimentation rate, and sedimentary organic matter in the
866 Oceans - I. Organic carbon preservation: *Deep-Sea Research* 26, 1347-1362.

867

868 Nielsen, J.K., Shen, Y., 2004. Evidence for sulfidic deep water during the Late Permian in the East
869 Greenland Basin. *Geology*, 32, 1037-1040.

870

871 Noble, R.A., Alexander, R., Kagi, R.I., Konx, J., 1986. Identification of some diterpenoid
872 hydrocarbons in petroleum. *Organic Geochemistry* 10, 825-829.

873

874 Oszczepalski, S., 1989. Kupferschiefer in southwestern Poland: sedimentary environment, metal
875 zoning, and ore controls. In: Boyle, R.W., Brown, A.C., Jowett, E.C., Kirkham, R.V. (Eds.),
876 Sediment-Hosted Stratiform Copper Deposits. Geological Association of Canada, Special Publication
877 36, 571-600.

878 Overmann, J., Cypionka, H., Pfenning, N., 1992. An extremely low-light-adapted phototrophic sulfur
879 bacterium from the Black Sea. *Limnology and Oceanography* 37, 150-155.

880 Pancost, R.D., Crawford, N., Maxwell, J.R., 2002. Molecular evidence for basin-scale photic zone
881 euxinia in the Permian Zechstein Sea. *Chemical Geology* 188, 217-227.

882 Paul, J., 2006. Der Kupferschiefer: Lithologie, Stratigraphie, Fazies and Metallogenese eines
883 Schwarzschiefers. *Zeitschrift der Deutschen Gesellschaft für Geowissenschaften* 157, 57-76.

884 Pedersen, T.F., Calvert, S.E., 1990. Anoxia vs. productivity: what controls the formation of organic-
885 carbon-rich sediments and sedimentary rocks. *AAPG Bulletin* 74, 454-466.

886 Peryt, D., Woszczyńska, S., 2001. Rząd Foraminiferida Eichwald, 1830. In: Pajchlowa, M., Wagner, R.
887 (Eds.), *Budowa geologiczna Polski. Atlas skamieniałości przewodnich i charakterystycznych, część*
888 *1c*. Państwowy Instytut Geologiczny, Warszawa 3, 25–41.

889 Peryt, T.M., Peryt, D., 1977. Otwornice cechsztyńskie monokliny przedsudeckiej i ich paleoekologia.
890 *Annales de la Société Géologique de Pologne* 47, 301-326.

891 Peryt, T.M., Geluk, M.C., Mathiesen, A., Paul, J., Smith, K., 2010. Zechstein. In: Doornenbal, J.C.
892 and Stevenson, A.G. (Eds.), *Petroleum Geological Atlas of the Southern Permian Basin Area*. EAGE
893 Publications, Houten, 123-147.

894 Peryt, T.M., Hałas, S., Peryt, D., 2015. Carbon and oxygen isotopic composition and foraminifers of
895 condensed basal Zechstein (Upper Permian) strata in western Poland: environmental and stratigraphic
896 implications. *Geological Journal* 50, 446-464.

897

898 Peters, K.E., Walters, C.C., Moldowan, J.M., 2005. *The Biomarker Guide. Volume 2: Biomarkers and*
899 *isotopes in petroleum exploration and Earth history*. Cambridge University Press, Cambridge.

900 Peters, K.E., Hostettler, F.D., Lorenson, T.D., Rosenbauer, R.J., 2008. Families of Miocene Monterey
901 crude oil, seep, and tarball samples, coastal California. AAPG Bulletin 92, 1131-1152.
902

903 Pletsch, T., Appel, J., Botor, D., Clayton, C., Duin, E., Faber, E., Górecki, W., Kombrink, H.,
904 Kosakowski, P., Kuper, G., Kus, J., Luts, R., Mathiesen, A., Ostertag-Henning, C., Papiernik, B., van
905 Bergen, F., 2010. Petroleum generation and migration. In: Doornenbal, J.C., Stevenson, A.G. (Eds.),
906 Petroleum Geological Atlas of the Southern Permian Basin Area. EAGE Publications b.v. (Houten),
907 pp. 225-253.
908

909 Pogge von Strandmann, P.A.E., Jenkyns, H.C., Woodfine, R.G., 2013. Lithium isotope evidence for
910 enhanced weathering during Oceanic Anoxic Event 2. Nature Geoscience 6, 668-672.
911

912 Repeta, D.J., 1993. A high resolution historical record of Holocene anoxygenic primary production in
913 the Black Sea. Geochimica et Cosmochimica Acta 57, 4337-4342.
914

915 Roscher, M., Stordal, F., Svensen, H., 2011. The effect of global warming and global cooling on the
916 distribution of the latest Permian climate zones. Palaeogeography, Palaeoclimatology, Palaeoecology,
917 309, 186-200.

918 Roveri, M., Taviani, M., 2003. Calcarene and sapropel deposition in the Mediterranean Pliocene:
919 shallow- and deep-water record of astronomically driven climatic events. Terra Nova 15, 279-286.
920

921 Sarmiento, J.L., Herbert, T.D., Toggweiler, J.R., 1988. Causes of anoxia in the world ocean. Global
922 Biogeochemical Cycles 2, 115-128.

923 Schobben, M., Stebbins, A., Ghaderi, A., Strauss, H., Korn, D., Korte, C., 2015. Flourishing ocean
924 drives the end-Permian marine mass extinction. PNAS 112, 10298-10303.
925

926 Schwark, L., Püttmann, W., 1990. Aromatic composition of the Permian Kupferschiefer in the Lower
 927 Rhine Basin, NW Germany. *Organic Geochemistry* 16, 749-761.

928 Schwark, L., Vliex, M., Karnin, W.-D., Waldmann, R., 1998. Geochemische Untersuchungen an
 929 ausgewählten Mutter- und Speichergesteinen des Zechsteins am Beispiel der Bohrung Sprötau Z1
 930 (Thüringer Becken). *Geologisches Jahrbuch A149*, 185-211.

931 Schwark, L., Empt, L., 2006. Sterane biomarkers as indicators of Palaeozoic algal evolution and
 932 extinction events. *Palaeogeography, Palaeoclimatology, Palaeoecology* 240, 225-236.

933

934 Schweitzer, H.-J., 1986. The land flora of the English and German Zechstein sequences. In: Harwood,
 935 G.M, Smith, D.B. (eds), *The English Zechstein and Related Topics*. Geological Society Special
 936 Publication 22, 31-54.

937 Şengor, A.M.C., Atayman, S., 2009. The Permian extinction and the Tethys: an exercise in
 938 global geology. *Geological Society of America, Special Papers* 448, 1-85.

939 Sinninghe Damsté, J.S., Wakeham, M.E., Kohnen, L., Hayes, J.M., de Leeuw, J.W., 1993. A 6,000-
 940 year sedimentary molecular record of chemocline excursions in the Black Sea. *Nature* 362, 827-829.

941 Sinninghe Damsté, J.S., Van Duin, A.C.T., Hollander, D., Kohnen, M.E.L., de Leeuw, J.W., 1995a.
 942 Early diagenesis of bacteriohopanepolyol derivatives: Formation of fossil homohopanoids.
 943 *Geochimica et Cosmochimica Acta* 59, 5141-5155.

944 Sinninghe Damsté, J.S., Kenig, F., Koopmans, M.P., Köster, J., Schouten, S., Hayes, J.M., de Leeuw,
 945 J.W., 1995b. Evidence for gammacerane as an indicator of water column stratification. *Geochimica et*
 946 *Cosmochimica Acta* 59, 1895-1900.

947

948 Sinninghe Damsté, J.S., Köster, J., 1998. A euxinic southern North Atlantic Ocean during the
 949 Cenomanian/Turonian oceanic anoxic event. *Earth and Planetary Science Letters* 158, 165-173.

950

951 Slach, J.-C., 1993. Die Beziehung zwischen der Organofazies und der Lithofazies/Paläogeographie
 952 für das Staßfurt-Karbonat (Ca₂) in Thüringen. Unveröffentlichte Diplomarbeit Universität zu Köln,
 953 58p.

954 Słowakiewicz, M., Tucker, M.E., Pancost, R.D., Perri, E., Mawson, M., 2013. Upper Permian
 955 (Zechstein) microbialites: Supratidal through deep subtidal deposition, source rock, and reservoir
 956 potential. AAPG Bulletin 97, 1921-1936.

957

958 Słowakiewicz, M., Tucker, M.E., Perri, E., Pancost, R.D., 2015. Euxinia in the photic zone of an
 959 ancient sea driven by a pronounced oxygen minimum zone. Palaeogeography, Palaeoclimatology,
 960 Palaeoecology 426, 242-259.

961 Smith, D.B., Taylor, J.C.M., 1992. Permian. In: Cope, J.C.W., Ingham, I.K., Rawson, P.F. (Eds.),
 962 Atlas of Palaeogeography and Lithofacies. Geological Society, London, Memoirs 13, 87-95.

963 Sørensen, S., Martinsen, B.B., 1987. A palaeogeographic reconstruction of the Rotliegendes deposit
 964 in the northeastern Permian Basin. In: Brooks, J., Glennie, K. (eds.) Petroleum Geology of NW
 965 Europe. Graham & Trotman, London, 497-508.

966 Stemmerik, L., Ineson, J.R., Mitchell, J.G., 2000. Stratigraphy of the Rotliegend Group in the Danish
 967 part of the Northern Permian Basin, North Sea. Journal of the Geological Society, 157, 1127-1136.

968 Strohmenger, C., Antonini, M., Jäger, G., Rockenbach, K., Strauss, C., 1996. Zechstein 2 Carbonate
 969 reservoir facies distribution in relation to Zechstein sequence stratigraphy (Upper Permian, northwest
 970 Germany): an integrated approach. Bulletin du Centre de recherches Exploration-Production Elf-
 971 Aquitaine, 20/1, 1-35.

972

973 Summons, R.E., Powell, T., 1986. Chlorobiaceae in Palaeozoic seas revealed by biological markers,
 974 isotopes and geology. Nature 319, 763-765.

975

976 Szurlies, M., 2013. Late Permian (Zechstein) magnetostratigraphy in Western and Central Europe. In:
 977 Gąsiewicz, A., Słowakiewicz, M. (Eds.) Palaeozoic Climate Cycles: Their Evolutionary and
 978 Sedimentological Impact. Geological Society, London, Special Publications 376, 73-85.
 979
 980 Tappan, H., 1980. The paleobiology of plant protists. W.H. Freeman and Company, San Francisco, p.
 981 1028.
 982
 983 Taylforth, J.E., McCay, G.A., Ellam, R., Raffi, I., Kroon, D., Robertson, A.H.F., 2014. Middle
 984 Miocene (Langhian) sapropel formation in the easternmost Mediterranean deep-water basin: Evidence
 985 from northern Cyprus. *Marine and Petroleum Geology* 57, 521-536.
 986
 987 Taylor, J.C.M., 1998. Upper Permian-Zechstein. In: Glennie, K.W. (ed.) *Petroleum Geology of the*
 988 *North Sea: Basic Concepts and Recent Advances*, Fourth Edition. Blackwell Science Ltd., pp. 174-
 989 211.
 990
 991 ten Haven, H.L., de Leeuw, J.W., Sinninghe Damsté, J.S., Schenck, P.A., Palmer, S.E., Zumberge,
 992 J.E., 1988. Application of biological markers in the recognition of palaeohypersaline environments.
 993 In: Fleet, A.J., Kelts, K., Talbot, M.R. (Eds.), *Lacustrine Petroleum Source Rocks*, Geological Society,
 994 London, Special Publications 40, 123-130.
 995
 996 ten Haven, H.L., Rohmer, M., Rullkötter, J., Bissleret, P., 1989. Tetrahymanol, the most likely
 997 precursor of gammacerane, occurs ubiquitously in marine sediments. *Geochimica et Cosmochimica*
 998 *Acta* 53, 3073-3079.
 999
 1000 Trendel, J.M., Restle, A., Connan, J., Albrecht, P., 1982. Identification of a novel series of tetracyclic
 1001 terpen hydrocarbons (C₂₄-C₂₇) in sediments and petroleums. *Journal of the Chemical Society,*
 1002 *Chemical Communications* 5, 304-306.

1003

1004 Turner, P., Magaritz, M., 1986. Chemical and isotopic studies of a core of Marl Slate from NE
 1005 England: influence of freshwater influx into the Zechstein Sea. In: Harwood, G.M., Smith, D.B. (Eds.),
 1006 The English Zechstein and Related Topics. Geological Society, London, Special Publications 22, pp.
 1007 19-29.

1008 Tyson, R.V., 1995. Sedimentary organic matter: Organic facies and palynofacies. Chapman and Hall,
 1009 615p.

1010 Uhl, D., 2004. Anatomy and taphonomy of a coniferous wood from the Zechstein (Upper Permian) on
 1011 NW-Hesse (Germany). *Geodiversitas* 26, 391-401.

1012 van Breugel, Y., Baas, M., Schouten, S., Mattioli, E., Sinninghe Damsté, J.S., 2006. Isorenieratane
 1013 record in black shales from the Paris Basin, France: constraints on recycling of respired CO₂ as a
 1014 mechanism for negative carbon isotope shifts during the Toarcian oceanic anoxic event.
 1015 *Paleoceanography* 21, PA4220.

1016

1017 van Wees, J.-D., Stephenson, R.A., Ziegler, P.A., Bayer, U., McCann, T., Dadlez, R., Gaupp, R.,
 1018 Narkiewicz, M., Bitzer, F., Scheck, M., 2000. On the origin of the Southern Permian Basin, Central
 1019 Europe. *Marine and Petroleum Geology* 17, 43-59.

1020

1021 Vella, A.J., Holzer, G., 1992. Distribution of isoprenoid hydrocarbons and alkylbenzenes in immature
 1022 sediments: evidence for direct inheritance from bacterial/algal sources. *Organic Geochemistry* 18,
 1023 203-210.

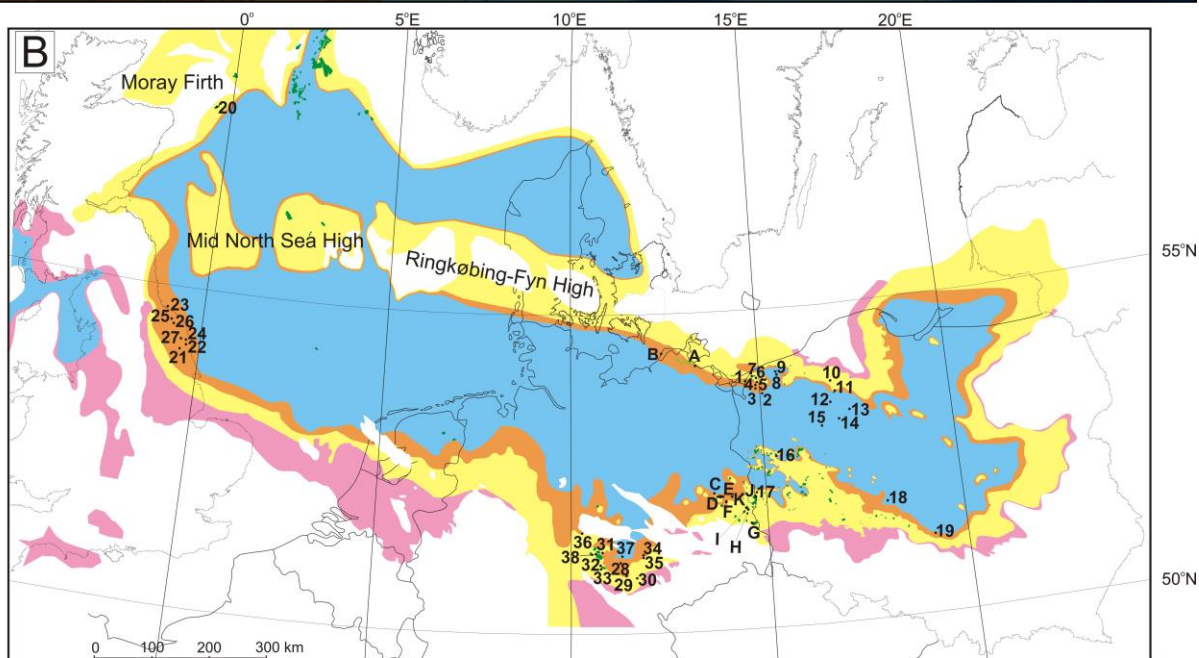
1024 Volkman, J., 1986. A review of sterol markers for marine and terrigenous organic matter. *Organic*
 1025 *Geochemistry* 9, 83-99.

1026 Volkman, J., Barrett, S., Blackburn, S., Mansour, M., Sikes, E., Gelin, F., 1998. Microalgal
 1027 biomarkers: a review of recent research development. *Organic Geochemistry* 29, 1163-1180.

1028 Wagner, T., Sinninghe Damsté, J.S., Hofmann, P., Beckmann, B., 2004. Euxinia and primary
 1029 production in Late Cretaceous eastern equatorial Atlantic surface waters fostered orbitally driven
 1030 formation of marine black shales. *Paleoceanography* 19, PA3009.
 1031 Weedon, G.P., Coe, A.L., Gallois, R.W., 2004. Cyclostratigraphy, orbital tuning and inferred
 1032 productivity for the type Kimmeridge Clay (Late Jurassic), Southern England. *Journal of the*
 1033 *Geological Society* 161, 655-666.
 1034 Wignall, P.B., Newton, R., 2001. Black shales on the basin margin: a model based on examples from
 1035 the Upper Jurassic of the Boulonnais, northern France. *Sedimentary Geology* 144, 335-356.
 1036 Williford, K.H., Grice, K., Holman, A., McElwain, J.C., 2014. An organic record of terrestrial
 1037 ecosystem collapse and recovery at the Triassic-Jurassic boundary in East Greenland. *Geochimica et*
 1038 *Cosmochimica Acta* 127, 251-263.
 1039
 1040 Ziegler, M.A., Hulver, M.L., Rowley, D.B., 1997. Permian world topography and climate. In: Martini,
 1041 I.P. (ed.), *Late Glacial and Post-glacial Environmental Changes: Quaternary, Carboniferous-Permian*
 1042 *and Proterozoic*. Oxford University Press, Oxford, pp. 111-146.
 1043
 1044 Zielinski, G.W., Poprawa, P., Szewczyk, J., Grotek, I., Kiersnowski, H., Zielinski, R.L.B., 2012.
 1045 Thermal effects of Zechstein salt and the Early to Middle Jurassic hydrothermal event in the central
 1046 Polish Basin. *AAPG Bulletin* 96, 1981-1996.
 1047
 1048 Figure caption



1049



1050

sabkha & salina
 platform
 slope
 basin
 highs/land
 petroleum accumulations

1051 Fig. 1. (A) Palaeogeography of the northern Pangea in Late Permian time with Northern
1052 (NPB) and Southern (SPB) Permian basins (after Blakey, 2015). (B) Palaeoenvironmental
1053 map of the Ca2 in the Late Permian in Europe (after Słowakiewicz et al., 2015). Longitude
1054 and latitude are present day values. Wells: 1 – Wapnica-3, 2 – Błotno-3; 3 – Wysoka
1055 Kamieńska-8; 4 – Wysoka Kamieńska-2; 5 – Benice-1; 6 – Kamień Pomorski-Z2; 7 – Kamień
1056 Pomorski-Z4; 8 – Jarkowo-2; 9 – Petrykozy-4K; 10 – Bielica-2; 11 – Czarne-2; 12 – Okonek-
1057 1; 13 – Lipka-1; 14 – Złotów-2; 15 – Piła IG-1; 16 – Gorzów Wielkopolski-2; 17 – Miłów-1;
1058 18 – Florentyna IG-2; 19 – Gomunice-10; 20 – 20/2-2; 21 – Malton-1 and -4; 22 – Lockton-
1059 2a and -7; 23 – Bates Colliery B2 and B8; 24 – YP-11; 25 – Vane Tempest VT-11; 26 –
1060 Offshore Borehole – 1, 27 – Egton High Moor 1; 28 – Sprötau Z1; 29 – Mellingen 1/70, 30 –
1061 Jena 106/62; 31 – Straußfurt 8/70; 32 – Dachwig 2/71; 33 – Dachwig 1/70; 34 – Eckartsberga
1062 2/68; 35 – Eckartsberga 1/68; 36 – Aue 1; 37 – Sprötau 4/69; 38 – Tennstedt 1/69.

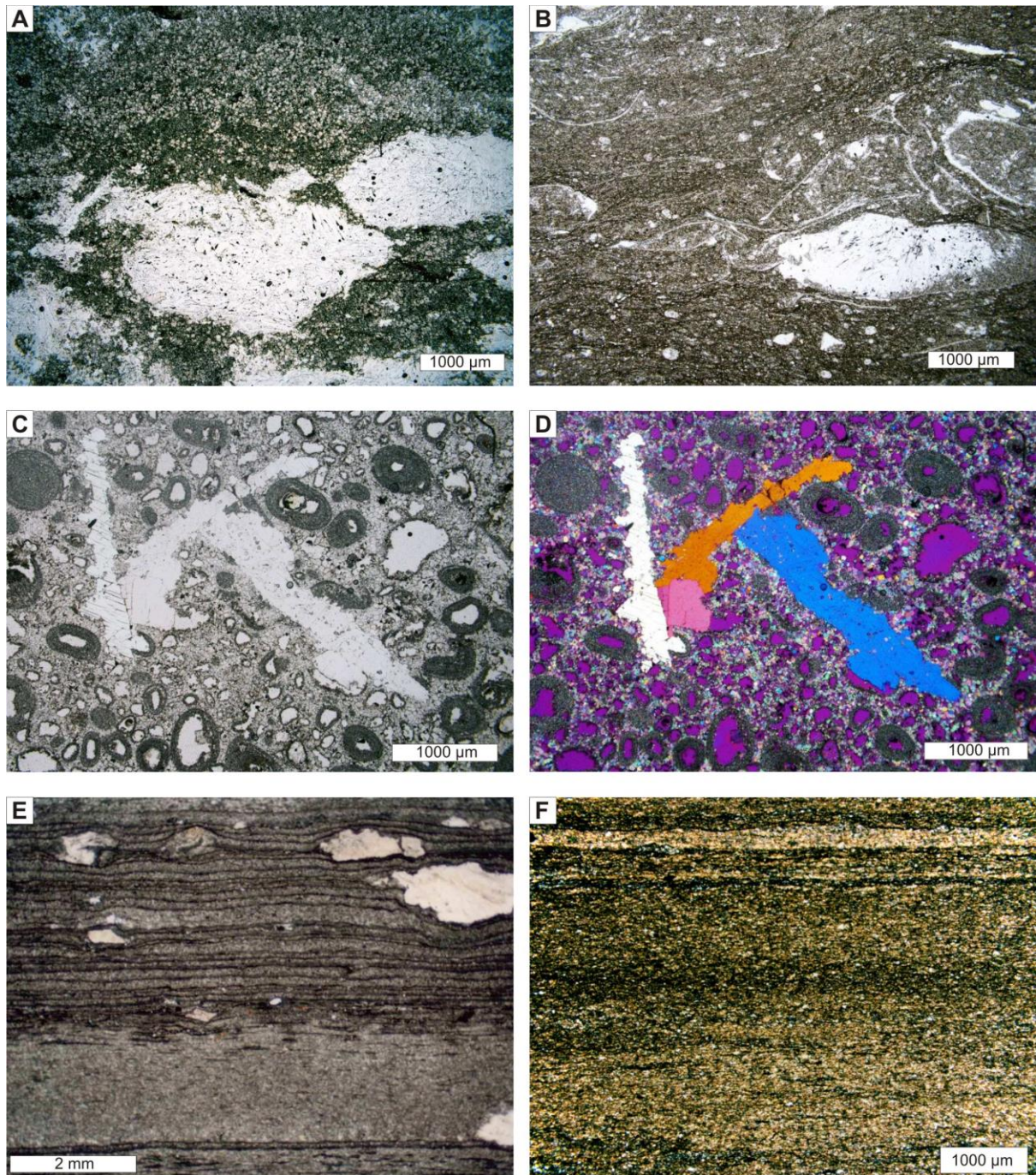


Fig. 2. Selected Ca₂ microfacies types. A. Peritidal facies: fine to coarse dolomite with small nodules composed of anhydrite after syn-sedimentary gypsum. Well: Offshore Borehole 1, NE England, depth 591 ft (181 m). B. Lagoonal facies: thin-shelled bivalves in a micritic sediment with calcispheres and foraminifera. Well: Miłów-1, SW Poland, depth 2030 m. C and D. Shelf-margin facies: oolitic grain- pack- stone with oomoldic porosity and some early

1069 (vadose) compaction and large replacement anhydrite crystals. Well: Malton 4, NE England,
1070 depth 4183 ft (1275 m). C – ppl; D – xp + tint. E. Lower slope facies: biolaminites and a thin
1071 fine-grained turbidite. Early diagenetic anhydrite is present within the laminites. Flakes of
1072 organic material occur within the upper part of the turbidite. Well VT-11, offshore Seaham,
1073 NE England, depth 317 ft (97 m). F. Basin facies: fine-grained carbonate with some more
1074 clay-organic-rich layers and a thin coarser lamina at the top (probably a very distal turbidite).
1075 Well: Piła IG-1, NW Poland, depth 4161.1 m.

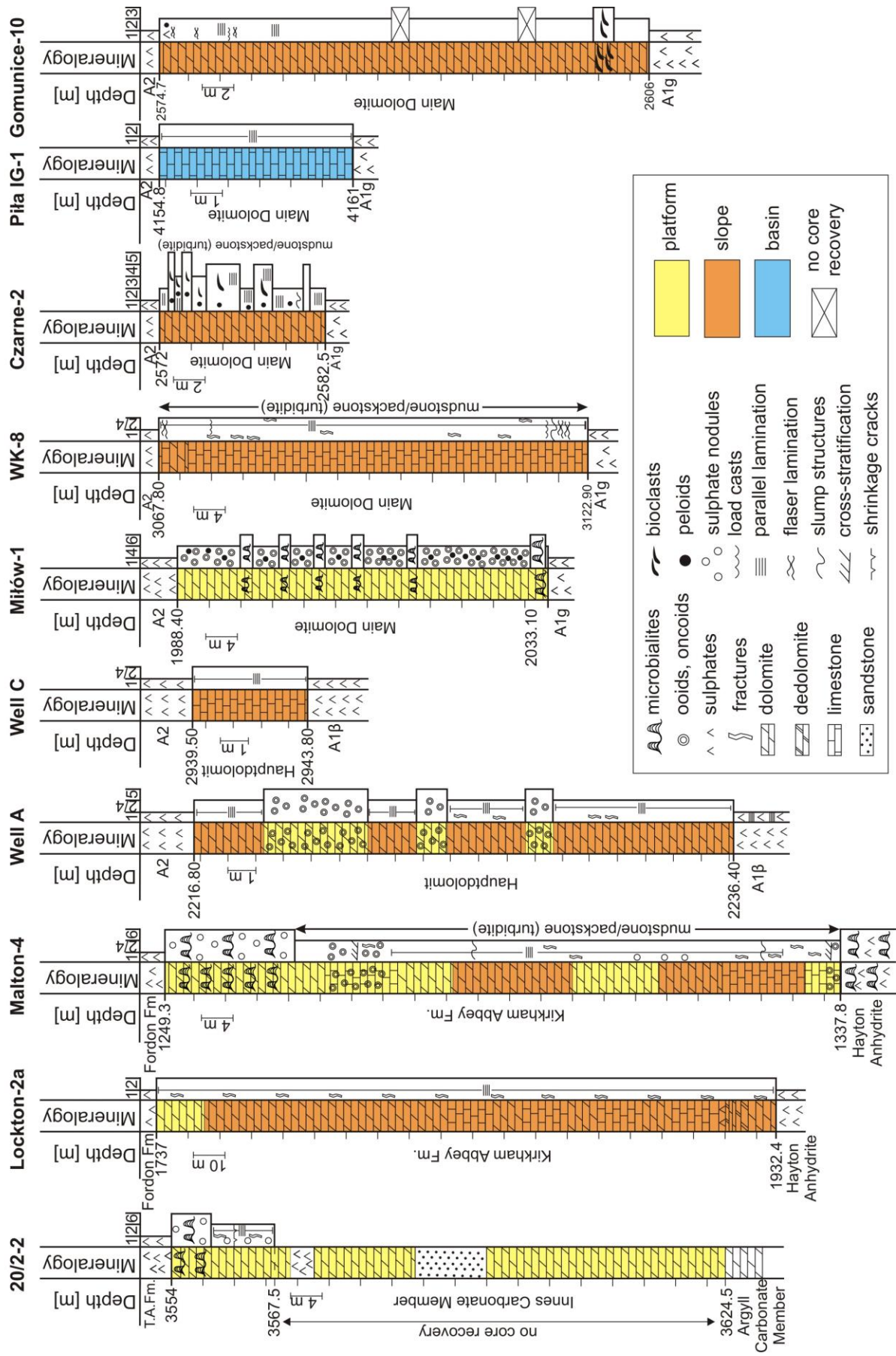


Fig. 3. Selected Ca2 (Innes Carbonate Member, Kirkham Abbey Fm., Hauptdolomit, Main Dolomite) wells from the Northern and Southern Permian basins. A1g, A1 β – Upper Anhydrite; Argyll Carbonate Member = Zechstein Limestone (Ca1); Hayton Anhydrite = Werra Anhydrite (A1). T.A.Fm. – Turbot Anhydrite Formation; 1 – anhydrite. Carbonate textures: 2 – mudstone, 3 – wackestone, 4 – packstone, 5 – grainstone, 6 – boundstone.

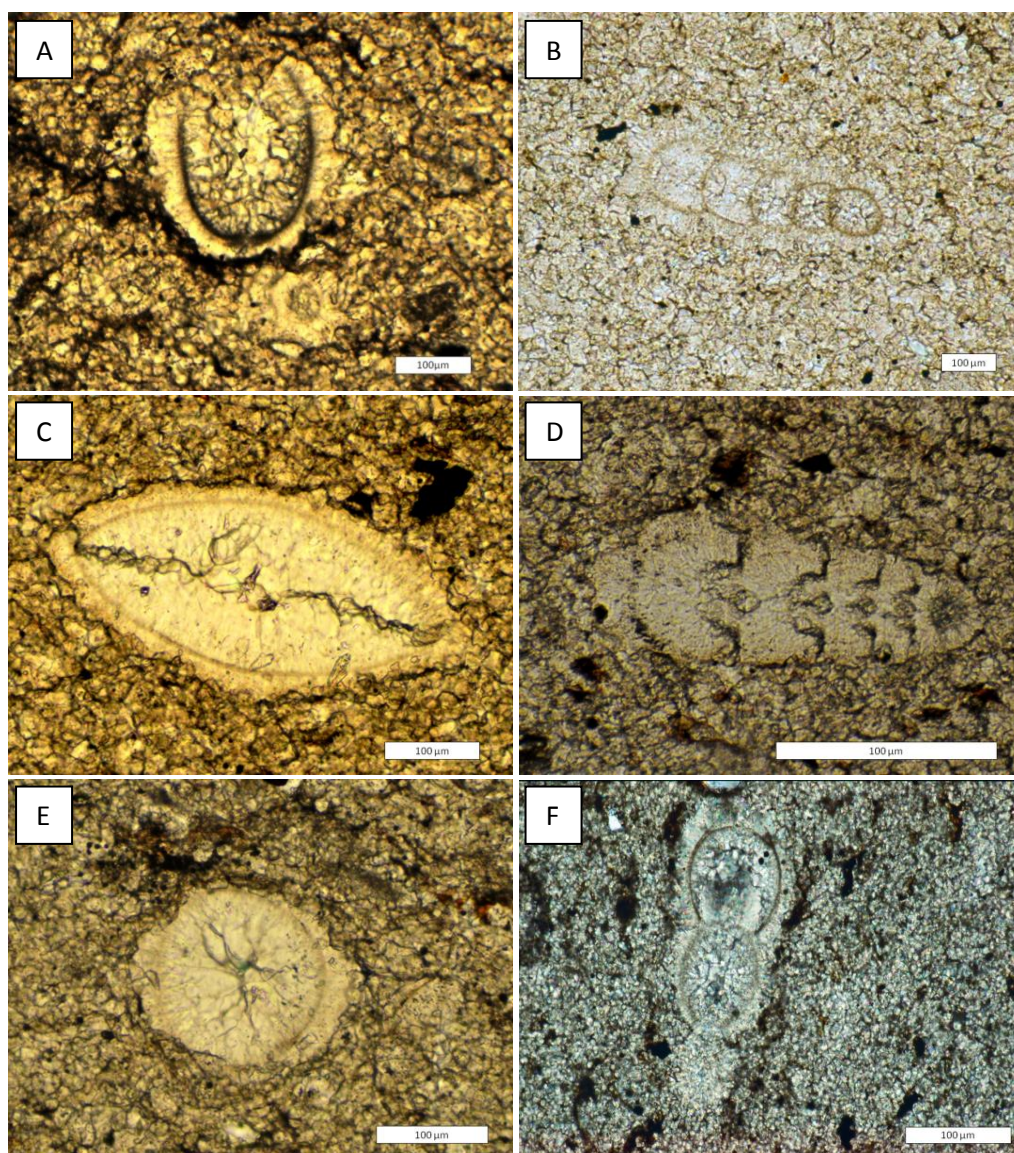
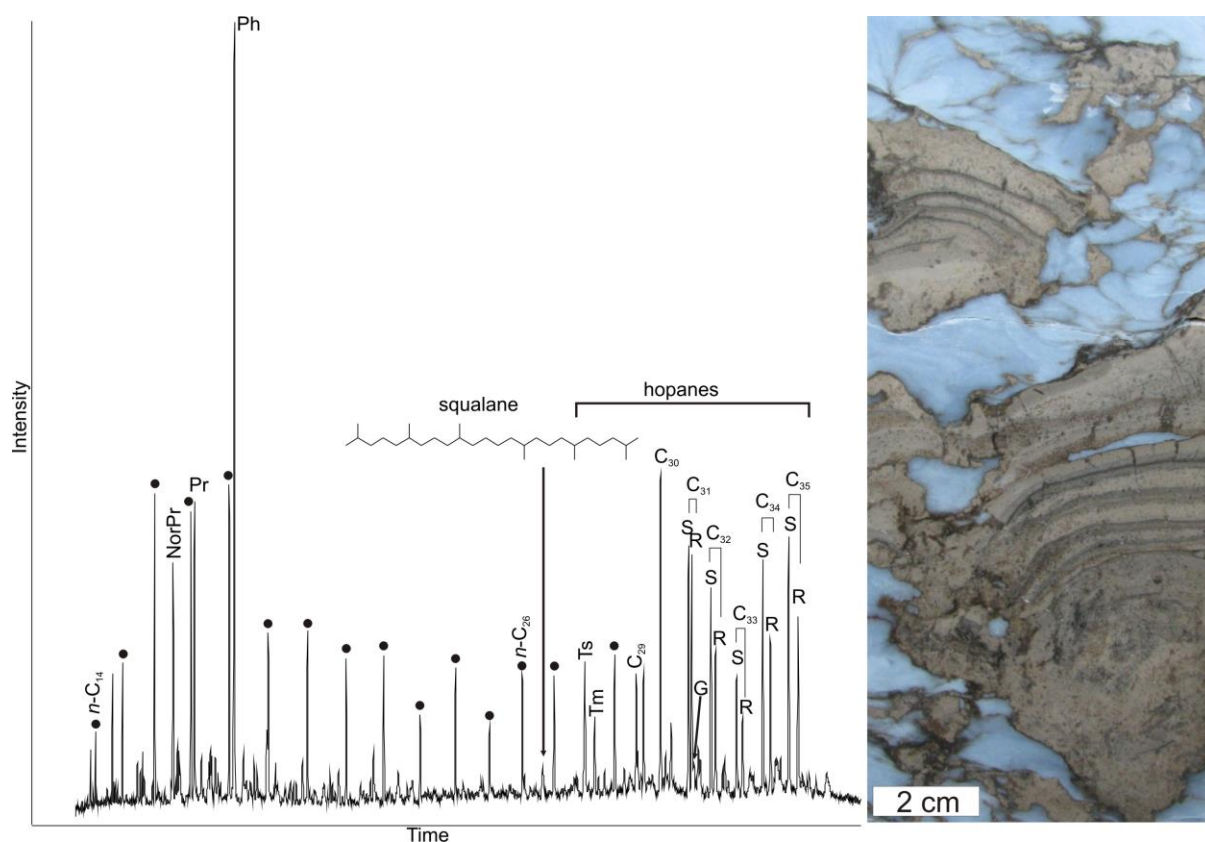


Fig. 4. Foraminifera and calcispheres from Ca2 lower slope facies of the well B. A) *Earlandia* sp., 2710.04 m; B) *Nodosaria* sp., 2707.93 m, C) Indeterminate foraminifera

1087 with terminal slit, 2707.93 m, D) *Polarisella* sp., 2707.93 m, E) *Calcispheres*, 2707.93 m, F)
 1088 *Nodosaria* sp., 2708.75 m.



1090 Fig. 5. Total ion current chromatogram of apolar fraction from the Ca2 stromatolites growing
 1091 within sulphates (anhydrite) in Offshore Borehole-1, depth 319.7 m (1049 ft). Note very high
 1092 abundance of pristane (Pr), phytane (Ph) ($Pr/Ph = 0.35$), and hopanes, which together with
 1093 the sedimentological evidence (presence of anhydrite) confirm evaporitic environment. NorPr
 1094 – norpristane; Ts – C_{27} 18 α -trisorhopane; Tm – 17 α -trisorhopane; G – gammacerane.
 1095 Black dots are *n*-alkanes.

NE SPB, NW Poland

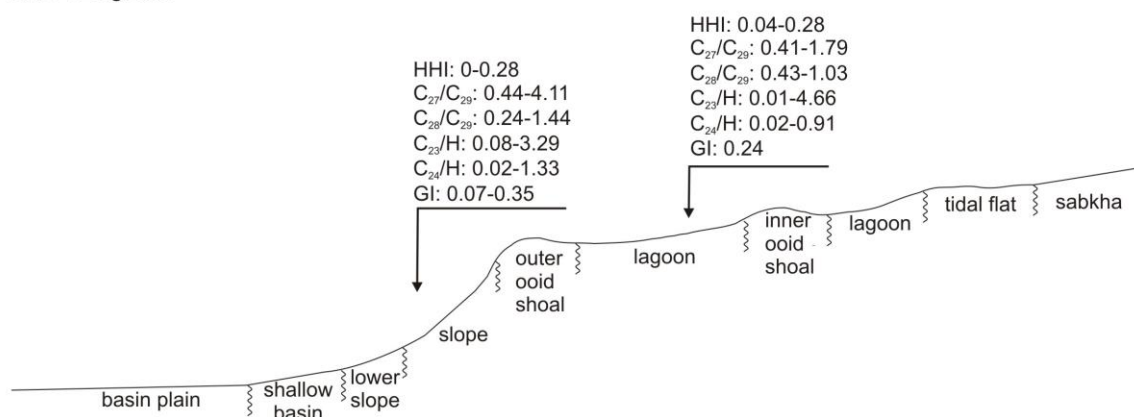


Diagram illustrating the relationship between geochemical data and coastal profile features. The profile shows a transition from basin plain to shallow basin, lower slope, outer ooid shoal, lagoon, inner ooid shoal, lagoon, tidal flat, and sabkha.

Geochemical data points (HHI, C_{27}/C_{29} , C_{28}/C_{29} , C_{23}/H , C_{24}/H , and GI) are plotted along the profile, indicating their distribution across different coastal features:

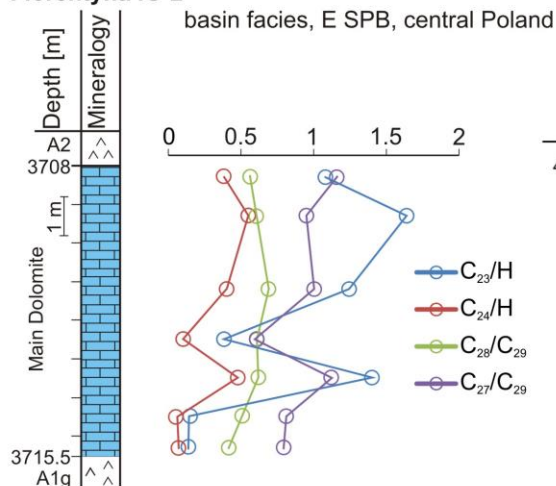
- Basin plain / Shallow basin / Lower slope:**
 - HHI: 0.08-0.19
 - C_{27}/C_{29} : 0.5-2.25
 - C_{28}/C_{29} : 0.26-0.84
 - C_{23}/H : 0.1-0.25
 - C_{24}/H : 0.09-0.41
- Outer ooid shoal:**
 - HHI: 0.06-0.09
 - C_{27}/C_{29} : 0.85-1.47
 - C_{28}/C_{29} : 0.5-1.03
- Lagoon (between outer ooid shoal and inner ooid shoal):**
 - HHI: 0.06-0.07
 - C_{27}/C_{29} : 0.4-0.78
 - C_{28}/C_{29} : 0.49-0.46
 - GI: 1-1.3
- Inner ooid shoal / Lagoon (between inner ooid shoal and tidal flat):**
 - HHI: 0.03-0.06
 - C_{27}/C_{29} : 0.5-1.28
 - C_{28}/C_{29} : 0.28-0.61
 - GI: 0.12-0.63
- Tidal flat / Sabkha:**
 - HHI: 0.04-0.4
 - C_{27}/C_{29} : 0.39-1.25
 - C_{28}/C_{29} : 0.31-0.61
 - C_{23}/H : 0.06-0.16
 - C_{24}/H : 0.06-0.31
 - sporadic isorenieratane & chlorobactane

W SPB, NE England

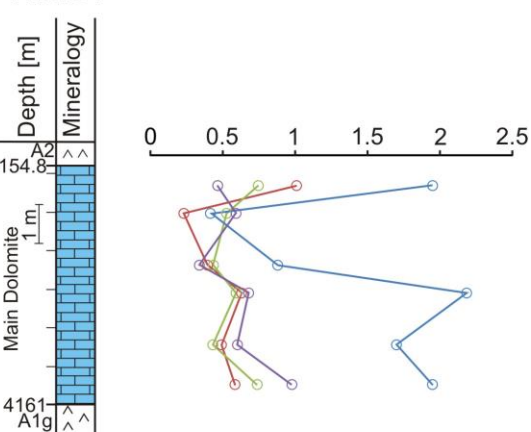


1097 Fig. 6. Biomarker parameters in the extractable organic matter obtained from the lagoonal-
1098 ooid shoal-slope-basin facies of the Southern Permian Basin (SPB) in Europe. Note
1099 biomarker differences in NE (a) SE (b) and W (c) SPB. Explanations of biomarkers are given
1100 in Table 1.

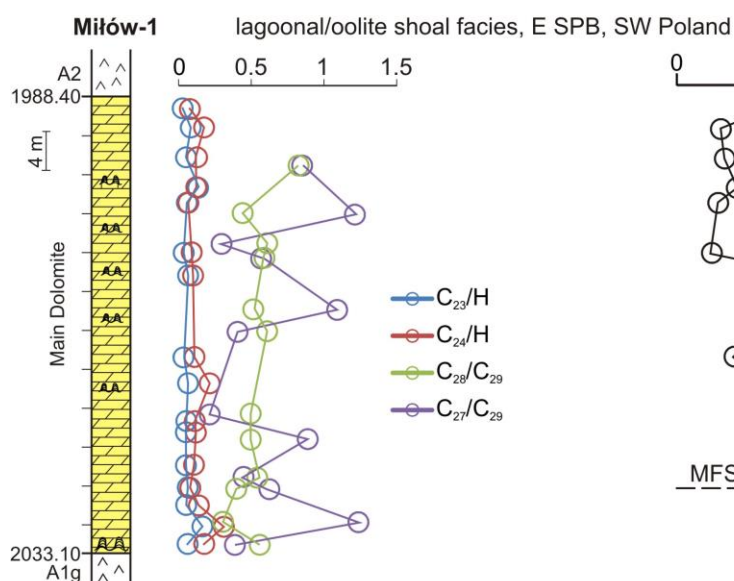
Florentyna IG-2



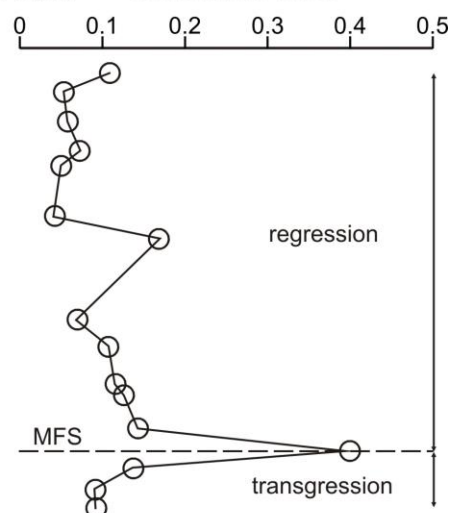
Piła IG-1



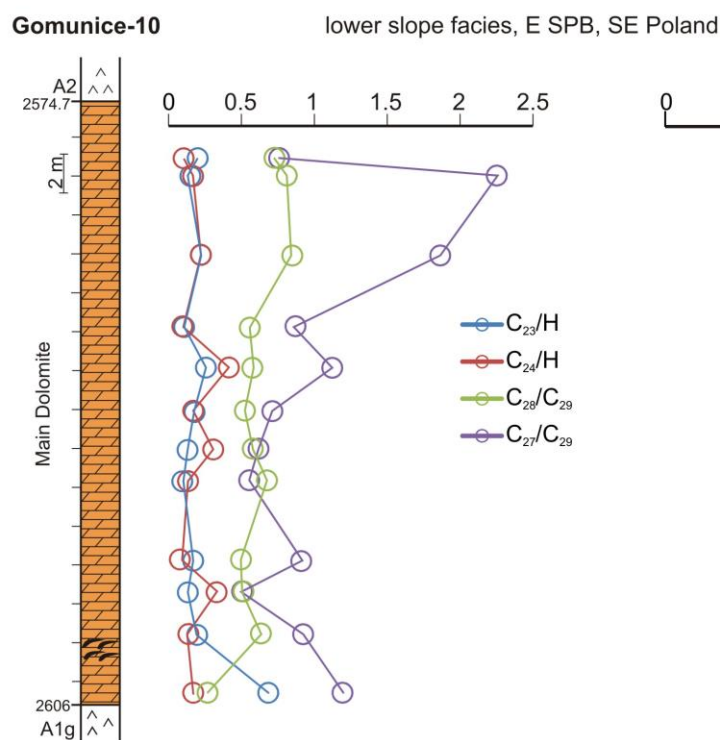
Miłów-1



homohopane index



Gomunice-10



homohopane index

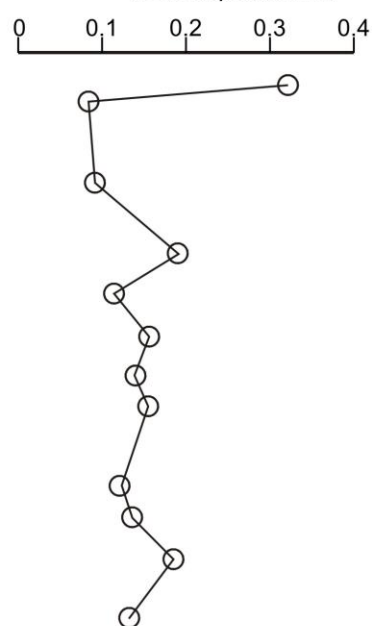


Fig. 7. Selected biomarker data in the extractable organic matter of the Florentyna IG-2 basin facies, Miłów-1 lagoonal/oolite shoal facies, and Gomunice-10 lower slope facies in E SPB. Explanations of biomarkers are given in Table 1. MFS – maximum flooding surface.

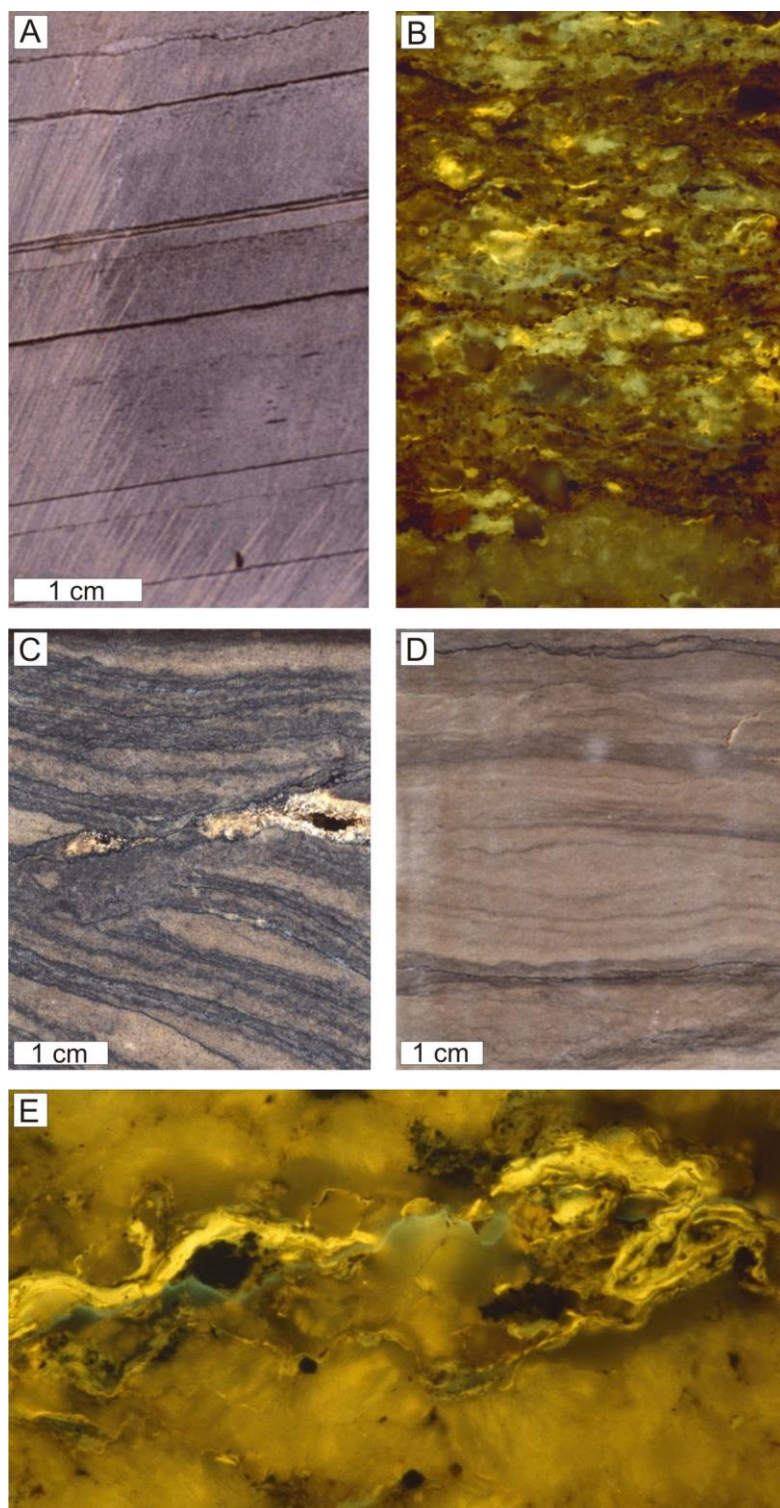


Fig. 8. Lower slope (A) typical laminated (black) and fine-grained turbiditic beds (light grey) in dolomudstone, well A, depth 2227.90 m; (C) and (D) laminated algal-microbial (dark laminae) interbedded with grey micritic layers, dolomudstone: (C) well J, depth 1944.94 m, (D) well I, depth 1974.5 m. Photomicrographs of macerals in UV light (pictures width is 0.28 mm): (B) liptinite (gold) in (A); and (E) lamalginite (gold) in (C), lagoonal facies.

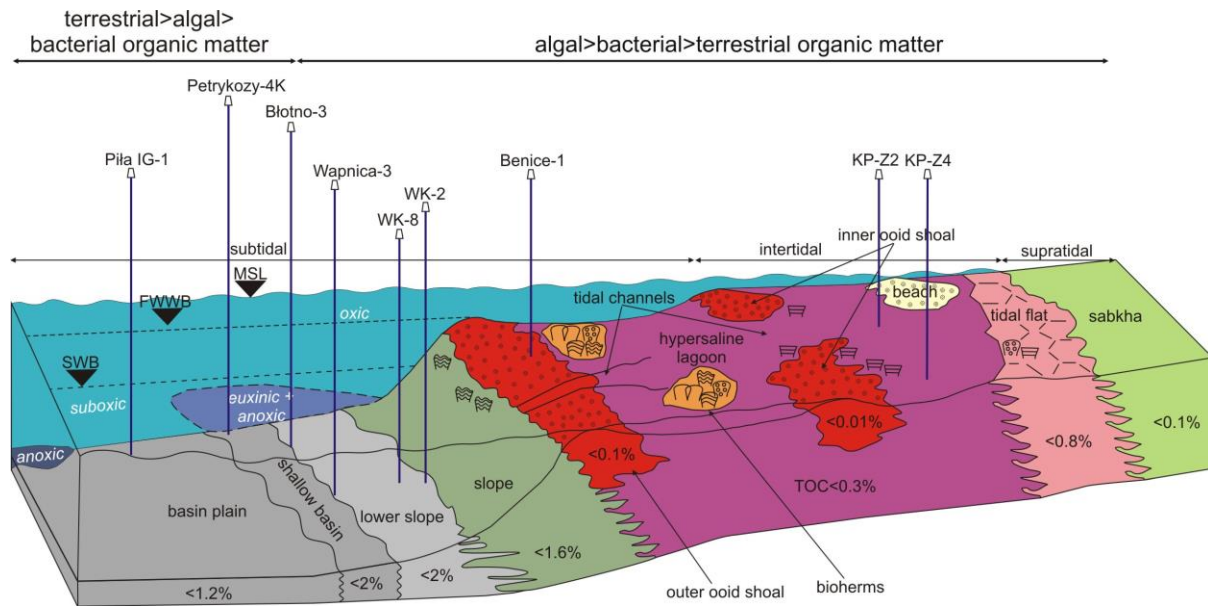
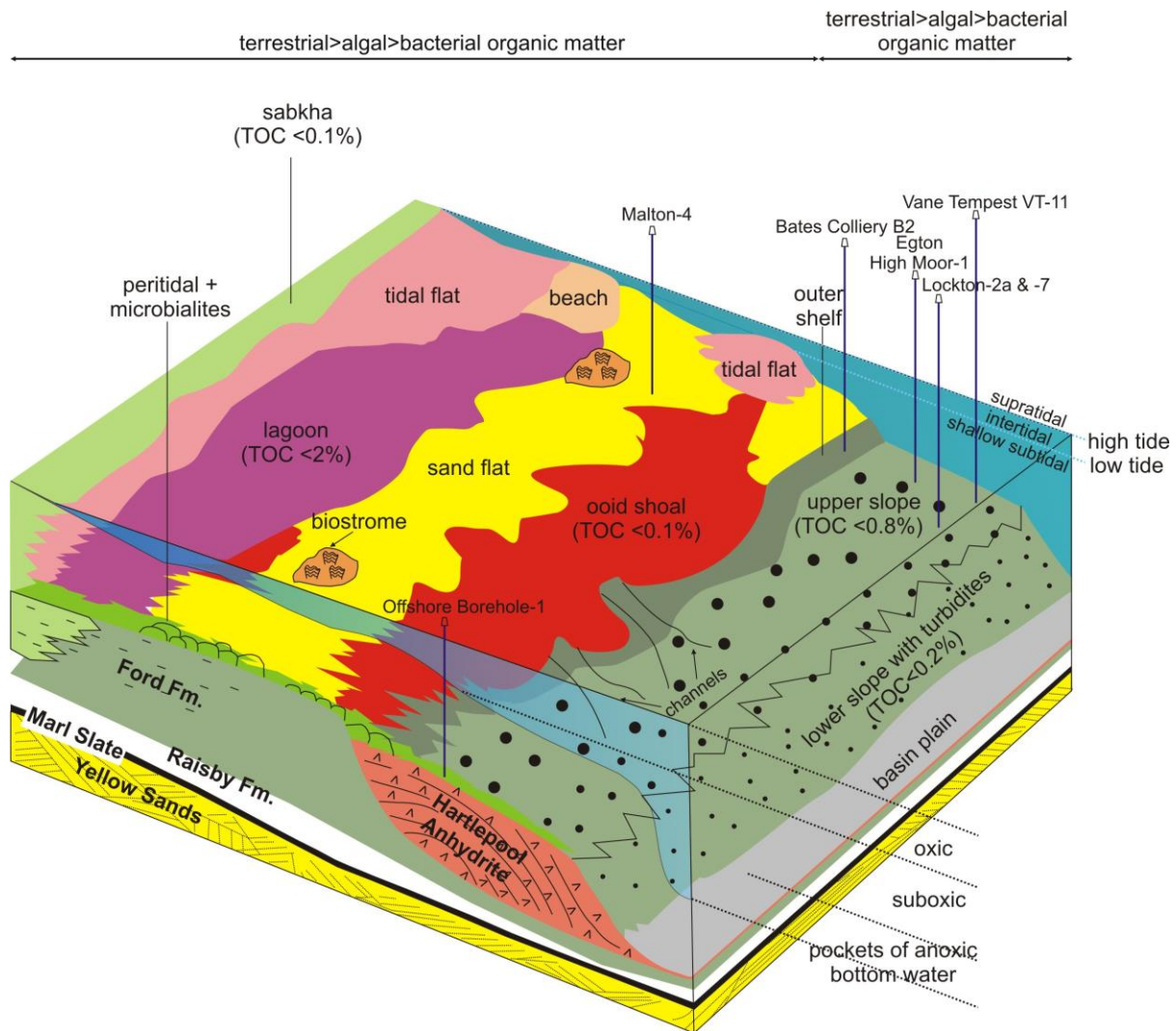


Fig. 9. General depositional models of the northeastern-central margin of the Southern Permian Basin in Ca2 time during sea-level highstand. MSL - mean sea level, FWWB - fair-weather wave base, SWB - storm wave base. Depositional model not to scale. TOC contents are maximum values.



1116

1117 Fig. 10. General depositional model of the western margin of the Southern Permian Basin in
 1118 Ca2 time during sea-level highstand. Depositional model not to scale. TOC contents are
 1119 maximum values.

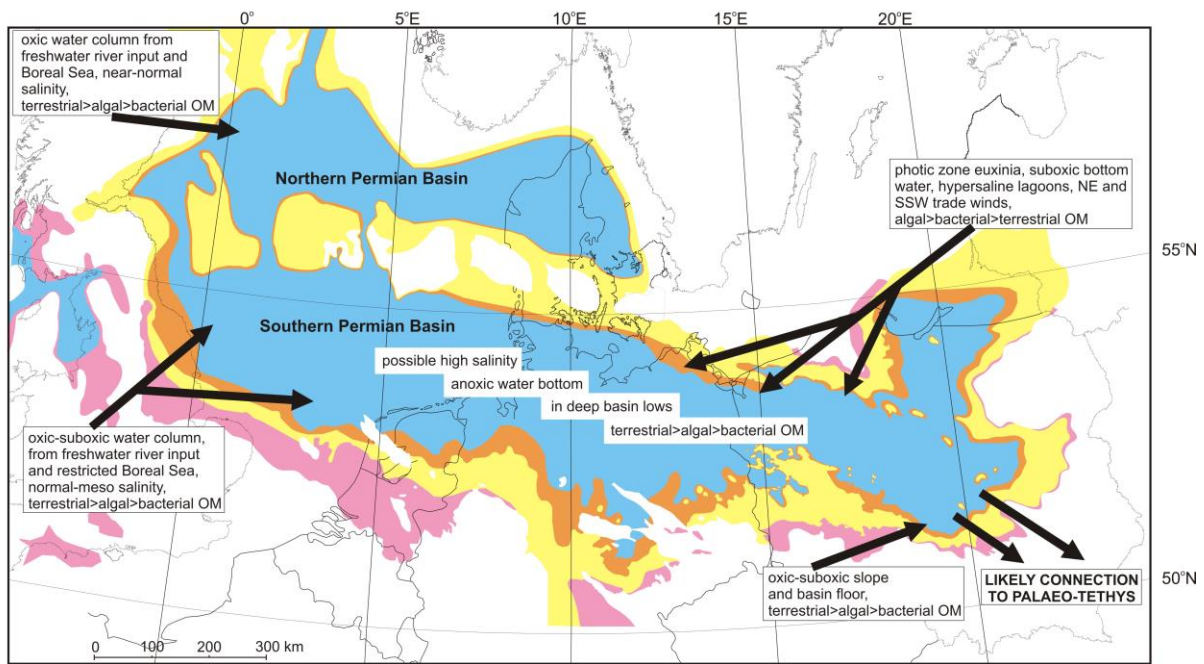


Fig. 11. Summary of palaeoceanographical conditions in the Northern and Southern Permian basins in Late Permian time. OM – organic matter. Colours as in Figure 1b.

Table 1. Summary of biomarker abundances and ratio measurements for compounds discussed in the text. nd – not determined. Biomarkers from Gorzów Wlkp-2, Lipka-1, Okonek-1, Złotów-2, and well L were not used due to high degradation of organic matter or high organic matter maturity ($VR_o = 1.2-1.4\%$). Numerator gives range of values and denominator gives average values.

Well (samples)	HHI ^a	C ₂₇ /C ₂₉ ^b	C ₂₈ /C ₂₉ ^c	C ₂₃ /H ^d	C ₂₄ /H ^e	GI ^f	C ₂₉ ^g	C ₂₈ ^g	C ₂₇ ^g
west margin of the NPB									
20/2-2 (6)	$\frac{0 - 0.08}{0.03}$	$\frac{0.68 - 1.18}{0.94}$	$\frac{0.62 - 0.79}{0.73}$	$\frac{0.05 - 1.46}{0.56}$	$\frac{0.03 - 0.8}{0.3}$	nd	$\frac{36 - 41}{38}$	$\frac{22 - 31}{27}$	$\frac{28 - 42}{35}$
west margin of the SPB									
B2 (1)	0.09	0.56	0.24	0.78	0.22	0.07	55	14	31
Egton High	0	$\frac{0.7 - 1.51}{1.11}$	$\frac{0.43 - 0.51}{0.47}$	$\frac{0.26 - 0.49}{0.26}$	$\frac{0.17 - 0.76}{0.76}$	nd	$\frac{33 - 47}{40}$	$\frac{17 - 20}{18}$	$\frac{33 - 50}{42}$
Moor-1 (3)									
Lockton 2a (4)	0	$\frac{1.92 - 4.11}{3.02}$	$\frac{0.78 - 1.44}{1.11}$	$\frac{1.36 - 3.29}{2.53}$	$\frac{0.5 - 1.33}{0.88}$	nd	$\frac{15 - 27}{21}$	$\frac{21 - 29}{22}$	$\frac{44 - 63}{57}$
Lockton 7 (1)	0	1.65	1.1	1.28	0.98	nd	27	29	44
Malton-4 (14)	$\frac{0.08 - 0.28}{0.21}$	$\frac{0.74 - 1.79}{1.23}$	$\frac{0.59 - 1.03}{0.89}$	$\frac{0.23 - 4.66}{1.67}$	$\frac{0.14 - 0.91}{0.34}$	nd	$\frac{27 - 42}{34}$	$\frac{24 - 28}{26}$	$\frac{31 - 47}{40}$
Offshore	$\frac{0.04 - 0.1}{0.07}$	0.41	0.43	$\frac{0.01 - 0.75}{0.38}$	$\frac{0.02 - 0.17}{0.1}$	0.24	54	23	33
Borehole 1 (2)									
Vane Tempest	0.28	0.44	0.74	0.08	0.02	0.35	46	34	20
VT-11 (2)									
north margin of the SPB									
Benice-1 (8)	$\frac{0.09 - 0.15}{0.11}$	$\frac{0.64 - 1.65}{0.96}$	$\frac{0.53 - 0.93}{0.72}$	$\frac{0.1 - 0.47}{0.28}$	$\frac{0.06 - 0.2}{0.15}$	nd	$\frac{31 - 43}{38}$	$\frac{19 - 33}{27}$	$\frac{26 - 51}{35}$
Bielica-2 (7)	$\frac{0.03 - 0.07}{0.05}$	$\frac{0.64 - 1.31}{0.93}$	$\frac{0.37 - 0.7}{0.49}$	$\frac{0.01 - 0.12}{0.07}$	$\frac{0.04 - 0.07}{0.06}$	nd	$\frac{37 - 46}{42}$	$\frac{14 - 27}{20}$	$\frac{30 - 49}{38}$
Łłotno-3 (8)	$\frac{0.28 - 0.37}{0.33}$	$\frac{0.32 - 0.6}{0.43}$	$\frac{0.42 - 0.75}{0.61}$	$\frac{0.07 - 0.35}{0.18}$	$\frac{0.08 - 0.14}{0.12}$	$\frac{0.33 - 0.49}{0.41}$	$\frac{42 - 56}{50}$	$\frac{23 - 35}{29}$	$\frac{17 - 26}{21}$
Czarne-2 (8)	$\frac{0.14 - 0.26}{0.22}$	$\frac{0.27 - 0.45}{0.37}$	$\frac{0.38 - 0.47}{0.44}$	$\frac{0.05 - 0.12}{0.08}$	$\frac{0.06 - 0.1}{0.07}$	$\frac{0.13 - 0.14}{0.14}$	$\frac{52 - 58}{55}$	$\frac{23 - 27}{24}$	$\frac{16 - 24}{21}$
Jarkowo-2 (7)	$\frac{0.16 - 0.34}{0.25}$	$\frac{0.68 - 1.18}{0.9}$	$\frac{0.54 - 0.77}{0.68}$	$\frac{0.07 - 0.22}{0.13}$	$\frac{0.14 - 0.24}{0.2}$	nd	$\frac{34 - 45}{39}$	$\frac{24 - 28}{26}$	$\frac{30 - 40}{35}$
KP-Z2 (7)	$\frac{0.04 - 0.08}{0.06}$	$\frac{0.38 - 0.95}{0.61}$	$\frac{0.27 - 0.84}{0.55}$	$\frac{0.01 - 0.38}{0.11}$	$\frac{0.1 - 0.25}{0.15}$	nd	$\frac{39 - 57}{47}$	$\frac{15 - 35}{25}$	$\frac{20 - 37}{28}$
KP-Z4 (12)	$\frac{0.05 - 0.21}{0.11}$	$\frac{0.44 - 0.94}{0.61}$	$\frac{0.41 - 0.74}{0.56}$	$\frac{0.03 - 0.19}{0.09}$	$\frac{0.04 - 0.14}{0.09}$	nd	$\frac{39 - 51}{46}$	$\frac{21 - 30}{26}$	$\frac{23 - 32}{28}$
Petrykozy-4K (7)	$\frac{0.22 - 0.3}{0.25}$	$\frac{0.78 - 1.02}{0.88}$	$\frac{0.66 - 0.76}{0.7}$	$\frac{0.08 - 0.17}{0.12}$	$\frac{0.19 - 0.36}{0.23}$	nd	$\frac{37 - 41}{39}$	$\frac{25 - 29}{27}$	$\frac{32 - 38}{34}$
Piła IG-1 (6)	nd	$\frac{0.46 - 0.97}{0.72}$	nd	$\frac{0.41 - 1.95}{1.08}$	$\frac{0.23 - 1}{0.54}$	nd	$\frac{37 - 45}{41}$	$\frac{27 - 34}{30}$	$\frac{21 - 36}{29}$
Wapnica-3 (8)	$\frac{0.33 - 0.48}{0.37}$	$\frac{0.31 - 0.62}{0.51}$	$\frac{0.3 - 0.5}{0.42}$	$\frac{0.03 - 0.07}{0.06}$	$\frac{0.04 - 0.07}{0.06}$	$\frac{0.16 - 0.33}{0.24}$	$\frac{47 - 62}{52}$	$\frac{19 - 24}{22}$	$\frac{20 - 30}{26}$
WK-2 (12)	$\frac{0.05 - 0.46}{0.3}$	$\frac{0.43 - 1.02}{0.64}$	$\frac{0.41 - 0.88}{0.61}$	$\frac{0.03 - 0.23}{0.1}$	$\frac{0.07 - 0.29}{0.12}$	$\frac{0.24 - 0.26}{0.25}$	$\frac{35 - 51}{45}$	$\frac{19 - 33}{27}$	$\frac{22 - 41}{28}$
WK-8 (24)	$\frac{0.2 - 0.56}{0.32}$	$\frac{0.26 - 0.73}{0.51}$	$\frac{0.35 - 0.94}{0.53}$	$\frac{0.02 - 0.45}{0.15}$	$\frac{0.01 - 0.72}{0.16}$	$\frac{0.14 - 1.0}{0.35}$	$\frac{38 - 61}{49}$	$\frac{18 - 36}{26}$	$\frac{16 - 30}{25}$

A (11)	$\frac{0.18 - 0.24}{0.21}$	$\frac{0.32 - 0.66}{0.71}$	$\frac{0.3 - 0.58}{0.6}$	nd	nd	nd	$\frac{45 - 62}{53}$	$\frac{19 - 26}{21}$	$\frac{27 - 30}{26}$
B (5)	$\frac{0.2 - 0.29}{0.25}$	$\frac{0.54 - 1.22}{0.88}$	0.44	nd	nd	nd	$\frac{38 - 50}{44}$	$\frac{17 - 22}{20}$	$\frac{27 - 46}{36}$
south margin of the SPB									
Florentyna IG-2 (8)	$\frac{0 - 0.1}{0.11}$	$\frac{0.59 - 1.16}{0.89}$	$\frac{0.42 - 0.69}{0.55}$	$\frac{0.14 - 1.64}{0.86}$	$\frac{0.32 - 0.52}{0.33}$	nd	$\frac{37 - 45}{41}$	$\frac{19 - 28}{23}$	$\frac{27 - 43}{36}$
Gomunice-10 (13)	$\frac{0.08 - 0.19}{0.15}$	$\frac{0.5 - 2.25}{1.02}$	$\frac{0.26 - 0.84}{0.6}$	$\frac{0.1 - 0.25}{0.16}$	$\frac{0.09 - 0.41}{0.2}$	nd	$\frac{25 - 45}{40}$	$\frac{11 - 30}{23}$	$\frac{25 - 55}{37}$
Miłów-1 (19)	$\frac{0.04 - 0.4}{0.11}$	$\frac{0.39 - 1.25}{0.69}$	$\frac{0.31 - 0.61}{0.53}$	$\frac{0.06 - 0.16}{0.07}$	$\frac{0.06 - 0.31}{0.13}$	nd	$\frac{37 - 58}{46}$	$\frac{12 - 32}{24}$	$\frac{13 - 49}{30}$
C (4)	$\frac{0.08 - 0.09}{0.09}$	$\frac{0.61 - 0.67}{0.63}$	$\frac{0.46 - 0.53}{0.5}$	nd	nd	$\frac{0.24 - 0.37}{0.3}$	$\frac{46 - 48}{47}$	$\frac{22 - 24}{23}$	$\frac{29 - 30}{30}$
D (1)	0.06	0.40	0.49	nd	nd	1	53	26	21
E (7)	$\frac{0.06 - 0.09}{0.08}$	$\frac{0.85 - 1.47}{1.26}$	$\frac{0.5 - 1.03}{0.8}$	nd	nd	$\frac{0.14 - 0.18}{0.16}$	$\frac{29 - 43}{33}$	$\frac{21 - 30}{26}$	$\frac{36 - 45}{41}$
F (1)	0.07	0.78	0.46	nd	nd	1.3	45	21	35
G (2)	0.06	$\frac{0.5 - 0.55}{0.53}$	$\frac{0.48 - 0.56}{0.52}$	nd	nd	$\frac{0.12 - 0.28}{0.2}$	$\frac{47 - 51}{49}$	$\frac{24 - 26}{25}$	$\frac{25 - 26}{26}$
H (7)	$\frac{0.03 - 0.05}{0.04}$	$\frac{0.81 - 1.28}{1.05}$	$\frac{0.37 - 0.61}{0.56}$	nd	nd	$\frac{0.14 - 0.44}{0.31}$	$\frac{35 - 43}{39}$	$\frac{14 - 28}{21}$	$\frac{34 - 48}{40}$
I (7)	0.05	$\frac{0.8 - 0.87}{0.84}$	$\frac{0.28 - 0.32}{0.3}$	nd	nd	$\frac{0.37 - 0.63}{0.5}$	$\frac{46 - 48}{47}$	$\frac{13 - 15}{14}$	$\frac{39 - 40}{39}$
J (7)	$\frac{0.03 - 0.06}{0.05}$	$\frac{0.69 - 0.77}{0.73}$	$\frac{0.44 - 0.45}{0.45}$	nd	nd	$\frac{0.18 - 0.19}{0.19}$	$\frac{45 - 47}{46}$	$\frac{20 - 21}{21}$	$\frac{32 - 35}{33}$

1129

1130 Table 2. Bulk isotopic data for the lagoonal, slope and basin plain facies representing northern
1131 margin of the Z2C sea are compiled (Słowakiewicz et al., 2015) and extended results. The upward-
1132 increasing $\delta^{13}\text{C}$ trend in the WK-8, Czarne-2 and Gomunice-10 wells from the northeastern (NW
1133 Poland) and southeastern (SE Poland) SPB suggests basin-wide increased productivity through the
1134 Z2C in platform margin-slope locations; this contrasts with the $\delta^{13}\text{C}$ record in the basin centre (Piła
1135 IG-1) where no trend is observed. Extra positive values of $\delta^{13}\text{C}$, as at the base of Malton-4 (+8.0‰,
1136 lagoonal facies, NE England), and also in the basal third Zechstein carbonate cycle (Z3C) in 20/02-2
1137 (8.9‰, lagoonal facies, our unpublished data), both of which are closely associated with anhydrite,

1138 may relate to increased salinity and evaporation (Lazar and Erez, 1990; Hendry and Kalin, 1997;
 1139 Gąsiewicz, 2013), although in the case of Lockton-2a, they could reflect a burial diagenetic, even
 1140 hydrothermal origin. The $\delta^{18}\text{O}$ data show variations in space and time, and these were partly the result
 1141 of changes in the $\delta^{18}\text{O}_{\text{SMOW}}$ composition of seawater as a result of fluctuations in evaporation-salinity
 1142 and freshwater input, resulting from the restricted nature of the basin, and the proximity to
 1143 connections to the more open oceans, Panthalassa to the northwest and Palaeo-Tethys to the southeast.

1144

Well	Depth (m)	Depositional system	$\delta^{13}\text{C}$ (‰ PDB)	$\delta^{18}\text{O}$ (‰ PDB)
Czarne-2	3572	lower slope	6.78	3.95
	3574		6.85	3.84
	3579		6.94	1.8
	3580		6.81	2.3
	3581		6.42	3.55
	3582		5.69	3.94
Ettrick 20/2-2	3554	lagoon	4.27	-11.26
	3554.8		5.59	-9.47
	3555		1.23	-11.65
	3556.7		5.24	-11.29
	3559		5.64	-5.26
Gomunice-10	2576.8	lower slope	6.6	0.81
	2585.9		6.6	0.82
	2588.1		6.79	0.92
	2592.5		6.62	0.51
	2602.5		5.9	1.57
	2605.7		5.93	-0.38
Lockton-2a	1915.7	upper slope	4.23	-13.95
	1920.8		3.92	-9.02
	1927		4.51	-3.35
	1930.6		2.61	-2.15
Malton-4	1253	lagoon	6.87	-0.92
	1255		6.84	-1.76
	1258.3		6.78	-2.32
	1258.8		6.98	-1.37
	1275		6.31	-2.19
	1293		6.16	-1.85
	1301		7.21	-1.54
	1316.7		7.15	-2.75
	1322.5		6.27	-1.36
	1325.8		6.31	-1.82
	1326.8		6.43	-1.99
	1334		6.25	-1.95
Piła IG-1	1341.4	basin plain	8.04	-0.55
	4155		5.22	-0.94
	4156		3.36	-1.05

	4158		4.74	-0.93
	4159		5.2	-0.83
	4160		4.91	-0.91
WK-8	3079.4	lower slope	6.33	1.85
	3085.4		6.44	2.50
	3092.5		6.39	2.32
	3097		6.22	2.26
	3100.3		6.23	2.02
	3109		5.71	2.48
	3111.5		5.68	2.17
	3113		6.18	1.23
	3116		5.83	1.31
	3122		4.48	1.07

1145

1146